UNIVERSITÀ DEGLI STUDI DI MODENA E REGGIO EMILIA

SCUOLA DI DOTTORATO IN MEDICINA MOLECOLARE E RIGENERATIVA

XXV CICLO

TESI DI DOTTORATO

ZFP36 expression impairs glioblastoma viability and invasiveness by targeting multiple signal transduction pathways.

Dottorando: Tommaso Selmi

Relatore: Dott. Tommaso Zanocco-Marani

Direttore/Coordinatore della scuola di dottorato:

Prof. Rossella Tupler

Anno Accademico 2012-2013

Table of Contents

1. ABSTRACT

The TIS11/TTP family of mRNA binding proteins regulates gene expression at the post-transcriptional level. Three members of this family have been described in humans: ZFP36, ZFP36L1 and ZFP36L2. TIS11/TTP proteins specifically recognize and bind adenine-uridine rich (AREII) sequences located in the 3'UTR of target messenger RNAs and once bound, TIS11/TTPs promote mRNA degradation via several mechanisms. Glioma is a primary brain tumor, characterized by high morbidity and mortality. At the molecular level is characterized by the activation of multiple signaling pathways that sustain resistance to apoptosis and promote survival and invasiveness. Among the players of this tumor are some oncogenes that carry AREII destabilizing sequences in their 3'UTR, such as the oncogenic kinases PIM1 and PIM3 and the x-linked inhibitor of apoptosis XIAP. Recent reports indicate that inhibition of XIAP sensitizes cells to pro-apoptotic therapy in glioma, while by inactivating PIM kinases it is possible to reduce the invasiveness of cancer cell lines. Here we show that ZFP36 is scarcely expressed in the glioma cell line ln827 and it exerts an anti tumoral activity when its expression is restored by retroviral transduction. The biological effects of ZFP36 expression have been described by mean of migration and anchorage independent growth assays and by Annexin V/ Propidium Idodide staining. Luciferase assays confirm that the AREII sequences located in the 3'UTR of PIM1, PIM3 and XIAP confer instability in presence of ZFP36. By Western Blot we show the activation of cell death programs

involving both apoptosis and necroptosis in cells over-expressing ZFP36. Taken together, our data show that it is possible to impinge on glioma cell lines viability and invasiveness by restoring the expression of ZFP36. Moreover, we provide evidence that compounds capable of inducing the expression of TIS11/TTP genes determine a comparable biological effect on the same cell contexts.

2. ARE-MEDIATED mRNA DECAY AND THE TIS11 FAMILY OF RNA BINDING PROTEINS

2.1 Messenger RNA turnover by Adenine-Uridine rich elements (ARE)

The control of messenger RNA (mRNA) turnover has a crucial role in regulating gene expression (Wilusz and Wilusz, 2004). mRNA stability is known to vary during processes such as differentiation and also in response to extracellular stimuli from pro inflammatory cytokines and during cellular stress. After being exported from the nucleus most mammalian mRNAs show a relatively long half-life (about 10 hours in mammalian cells), while a subset of other mRNAs decays more rapidly, their half-life ranging between 15 minutes and 2 hours. The rapid decay of this mRNA subset is determined by the presence of specific destabilizing motifs that are located in the 3' untranslated region (3'UTR). Among the regulatory motifs, AU-rich elements (ARE) are the most common, being present in about 8% of all mRNAs (Khabar, 2005). The ARE destabilizing signal recruits a set of RNA binding proteins (RBP) that target the mRNA to the cellular decay machinery where the ARE mediated decay (AMD) takes place (Fig.1).

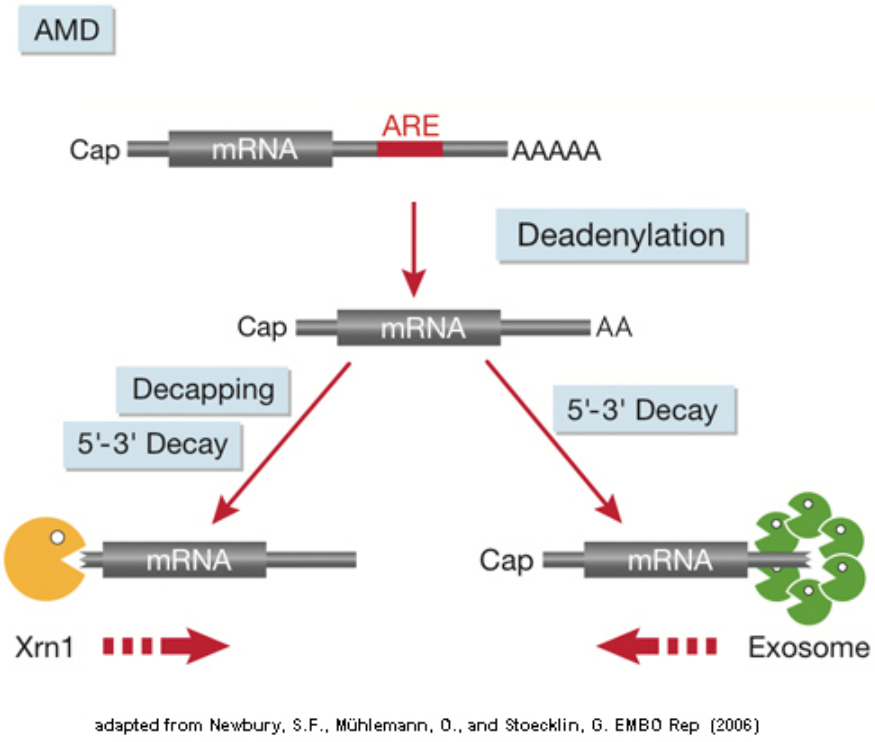

adapted from Newbury, S.F., Mühlemann, O., and Stoecklin, G. EMBO Rep (2006)

Fig.1: Scheme for the ARE-mediated mRNA decay (AMD). The regulation of gene expression involves the control of mRNA degradation at the post-transcriptional level. mRNAs containing an AU-rich element (ARE) in their 3′ untranslated region (UTR) undergo rapid ARE-mediated mRNA decay (AMD). The basic mRNA decay machinery in the cytoplasm initially removes the poly(A) tail through the activity of deadenylating enzymes. Subsequently, the mRNA can be further degraded from the 3′ end by a complex of 3′–5′ exonucleases known as the exosome. Alternatively, the mRNA is decapped at the 5′ end, and the 5′–3′ exonuclease Xrn1 proceeds to degrade the mRNA.

Molecular studies reveal that the first step of AMD in eukariotes is deadenylation. The shortening of the poly(A) tail is performed by at least three different complexes comprising deadenylating enzymes that are: the Ccr4–Not complex, the Pan2/3 complex and the poly (A)-specific ribonuclease (PARN). When the deadenylating step is completed, a complex of exonucleases and helicases, known as the exosome, degrades the mRNA in the 3′–5′ direction. At the 5′ end, the 7 methyl guanosine (7mG) cap is

removed by decapping enzymes, making it possible for the exoribonuclease Xrn1 to degrade the mRNA in the 5'-3' orientation.

2.2 ARE-carrying mRNAs

ARE-mRNAs are a heterogeneous group including regulators of pro-inflammatory response, of transcription, proliferation, RNA metabolism, and growth factor signaling (Tab.1). The basic ARE motif is an adenylate uridylate-rich sequence forming a pentamer AUUUA or the nonamer UUAUUUAUU. In non-AU contexts the pentameric sequence AUUUA is not functional, in fact, it is largely expressed in many mRNAs, regardless of the mRNA region, without affecting their stability. The nonamer, instead, is the most effective signal in inducing mRNA decay and is highly specific to the 3' UTR when compared to other regions of the mRNA (Khabar, 2010). Based on the kinetics of mRNA decay, ARE sequences have been divided in three classes: class I, that presents 1-3 repetitions of the AUUUA pentamer in a region rich in uridine residues, class II that has one or two overlapping copies of the nonamer UUAUUUAUU in an U rich region and class III, that is much less well defined, consisiting of U-rich regions not containing AUUUA motif (Chen and Shyu, 1995). Of these three classes, the third class is still poorly characterized, while much more is known about the first two. Recently, a complete database of AU-rich elements found in mRNAs (ARED) has been published online (http://brp.kfshrc.edu.sa/ARED/), based on a

computational analysis that considers the presence in the transcripts' 3' UTR of the minimal motif WWWT[ATTTA]TWWW (with one allowed mismatch outside of the bracketed region and where W is either an adenylate or an uridylate residue) (Bakheet et al., 2006).

2.3 TIS11 family of mRNA binding proteins

TIS11 family of RNA-binding proteins consists in humans of three members: ZFP36 (Zinc Finger Protein 36 C3H type homolog mouse, TTP, TIS11), ZFP36L1 (TIS11b, BRF-1) and ZFP36L2 (TIS11d, BRF-2). These zinc finger proteins are involved in the regulation of mRNA turnover directed by ARE elements (AMD). ZFP36 (in the figures referred to as TTP) was initially identified in cultured murine 3T3 fibroblasts treated with TPA (12-O-tetradecanoylphorbol-13-acetate), its mRNA showing the expression pattern of immediate-early response genes (Lai et al., 1990; DuBois et al., 1990). Two other mRNA sequences which displayed a similar trend in response to growth factors were later identified and called ZFP36L1 and ZFP36L2, these sequences share >70% amino acid identity to ZFP36 (Fig.2) (Varnum et al., 1991; Gomperts et al., 1992), for a review see Sanduja (Sanduja et al., 2012).

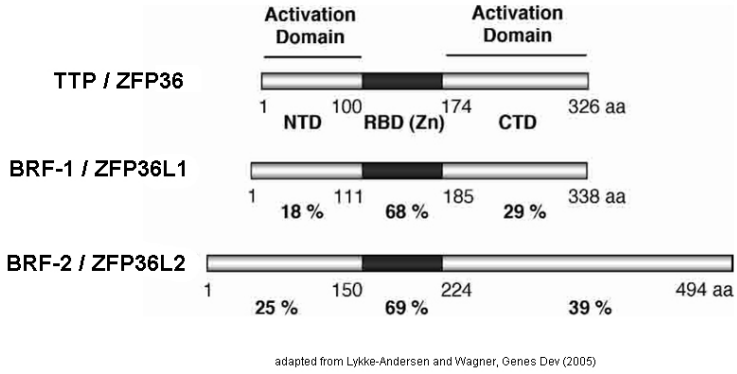

Fig.2 : Schematic representation of TTP (ZFP36), BRF-1 (ZFP36L1), and BRF-2 (ZFP36L2). The RNA-binding zinc-finger domain is shown in black (RBD- Zn). The N-terminal (NTD) and C-terminal (CTD) mRNA decay activation domains are shown in grey. The percent amino acid identity to TTP, of the NTD, RNA-binding domain, and CTD of BRF-1 and BRF-2 is given. (aa) Amino acids.

3. ZFP36: AN mRNA DESTABILIZING PROTEIN

3.1 ZFP36 gene and mRNA

In humans, ZFP36 gene is located on the chromosome 19q13.2 (http://genome.ucsc.edu/cgi-bin/hgTracks), and consists of two exons and one intron (DuBois et al., 1990). The promoter analysis of ZFP36 reveals a conserved 5'-proximal region that contains the consensus binding sites for several transcription factors, such as SP-1, AP-2 and EGR-1 (Lai et al., 1995). Another conserved region containing the consensus site for SP-1 is located in the single intron of ZFP36 gene and it has been shown that it cooperates with the promoter to drive the transcription of ZFP36, leading to a rapid increase in its mRNA levels as soon as 15 min after stimulation and returning to basal levels within 2 hours (Lai et al., 1998). This accounts for the serum-dependent induction of ZFP36, which was first observed at the time of its characterization as an early-immediate response gene to growth factors (Lai et al., 1990). In human T cells, the administration of Transforming Growth Factor Beta (TGFb) induces ZFP36 through the binding of Smad 3-4 transcription factors to responsive Smad binding-elements that are also present in its promoter (Ogawa et al., 2003). A last observation on ZFP36 gene structure regards the presence of a stretch of CpG islands that spans from the 5' proximal-promoter region to the first half of the second exon, this allowing epigenetic modifications of the DNA sequence that might influence ZFP36 transcription (Fig.1r). To date, no

evidences of these possible modifications have been collected. As regards transcription of ZFP36 gene, it has been shown that this is promoted by growth factors (e.g. EGF) and is part of a feedback inhibition mechanism that shuts down the response to growth factor signaling (Amit et al., 2007). Consistent with its role as quencher of cell activation, other studies have shown that also growth-inhibitory cytokines (e.g. TGF-beta, interferon) as well as anti-inflammatory hormones such as glucocorticoids, can promote ZFP36 transcription, suggesting that they control inflammatory response in part by ZFP36 expression (Ogawa et al., 2003; Ishmael et al., 2008).

ZFP36 messenger is 1745 bp long and contains in its 3'UTR the AU-rich elements that promote ARE-mediated mRNA decay, this allowing a rapid drop in the mRNA levels within 2-4 hours after transcriptional induction (Lai et al., 1990). By directly binding to these AU-rich elements, ZFP36 can auto-regulate the stability of its mRNA forming a feedback loop to limit expression levels. On the contrary, it has been shown that ZFP36 mRNA is stabilized by the activation of the p38 MAPK (Tchen, 2004).

3.2 ZFP36 and ARE-mediated mRNA decay

The main feature of ZFP36 protein is the presence of two conserved tandem zinc finger domains with identical Cx8Cx5Cx3H spacing, with 18 amino acids between the carboxyl terminal H of the first zinc finger and the amino terminal C of the second zinc finger (Lai et al., 1990). ZFP36 amino acid

sequence is rich in proline (16%) and serine (17.5%) residues and harbors a characteristic sequence of three PPPPG motifs (Lai et al., 1990). Structural and functional studies revealed that the integrity of ZFP36's tandem zinc fingers is necessary for its ability to bind to AU rich elements on target mRNAs and for promoting transcripts deadenylation (Lai et al., 1999). Characterized as a nuclear early-immediate response gene containing two Tandem Zinc Finger Domains (TZFD), ZFP36 was initially believed to be a transcription factor (Taylor et al., 1995; Taylor, 1996). Its ability to bind AU-rich elements and promote mRNA decay was discovered only after the generation of ZFP36 knockout mice (Taylor et al., 1996). The main feature of this strain of mice is the development of a systemic inflammatory syndrome, due to the over production of Tumor Necrosis Factor alpha (TNFa) (Taylor et al., 1996). Carballo and colleagues demonstrated that ZFP36 directly binds to AU-rich elements in the 3' UTR of the TNFa mRNA resulting in its rapid degradation and in ZFP36 knockout mice this ability is lost (Carballo et al., 1998), thus explaining the chronic inflammatory status of this mouse model. Molecular studies revealed that ZFP36 preferentially binds to the sequence 5'-UUAUUUAUU-3' which contains the core element 5'-UAUUUAU-3' (Brewer et al., 2004), that is found in many ARE carrying mRNAs (Lai et al., 1999; 2000). ZFP36 mutants that lack the CCCH residues in the TZFD cannot bind to ARE sequences contained in target mRNAs and exert a dominant-negative activity in vivo (Lai et al., 2002). Once bound to target mRNAs ZFP36 promotes poly(A) tail shortening and messenger degradation. In vitro, ZFP36 promotes poly(A) tail shortening in concert

with the poly(A)-specific ribonuclease (PARN) complex, however no direct interaction between the two proteins has been demonstrated (Lai et al., 2003). In vivo, ZFP36 interacts with the Caf1 deadenylase complex, suggesting that poly(A) shortening might result from the activity of this major mammalian deadenylating complex (Marchese et al., 2010). Recently it has been shown that the interaction between ZFP36 and Caf1 is mediated by the carbon catabolite repressor protein 4 (Ccr4)-Negative on TATA (Not1) complex (Sandler et al., 2011). Apart from its ability to interact with deadenylating enzymes, ZFP36 delivers bound mRNAs to the exosome (Chen et al., 2001) where rapid mRNA degradation takes place. This evidence demonstrates that ZFP36 enhances the 3'-5' decay of target mRNAs and interestingly also its involvement in the 5'-3' has been recently demonstrated. 5' – 3' decay starts with removal of 7-methyl guanosine cap by the decapping complex Dcp1/Dcp2, which promotes mRNA degradation by the 5'- 3' exonuclease Xrn1 (Cougot et al., 2004; Arribas-Layton et al., 2012). The components of the 5'- 3' decay complex co-localize at small cytoplasmic foci known as processing (P)-bodies (PBs), which also contain factors involved in translational silencing, and miRNA- and siRNA-mediated mRNA silencing (Arribas-Layton et al., 2012; Pillai, 2005). When associated with components of the decapping machinery such as Hedls, hEdc3, Dcp1/Dcp2 and Xrn1, ZFP36 can promote the degradation of ARE mRNAs in the processing bodies (Lykke-Andersen and Wagner, 2005) (Fenger-Grøn et al., 2005; Hau et al., 2007). It has been demonstrated that in experimental conditions, ZFP36 over-expression promotes P-body formation and relocates

ARE-mRNAs from the polysomes to the P-bodies. Physiologically, the assembly of P-bodies is an event that occurs when the cellular mRNA decay components are limiting (Franks and Lykke-Andersen, 2007). ZFP36 can also localize into small cytoplasmic structures called stress granules (SGs) (Murata et al., 2005), that assemble in response to cellular stress and contain translation arrested mRNAs and ARE-binding proteins (ABP) (Anderson and Kedersha, 2006; 2008). Given the ability of ZFP36 to shuttle between P-bodies and SG it is conceivable that depending on the cellular status (energetic, metabolic, resting/activation) ZFP36 shuttles ARE-mRNAs targeted for disruption or translational arrest between these two organelles (Kedersha et al., 2005) (Fig.3).

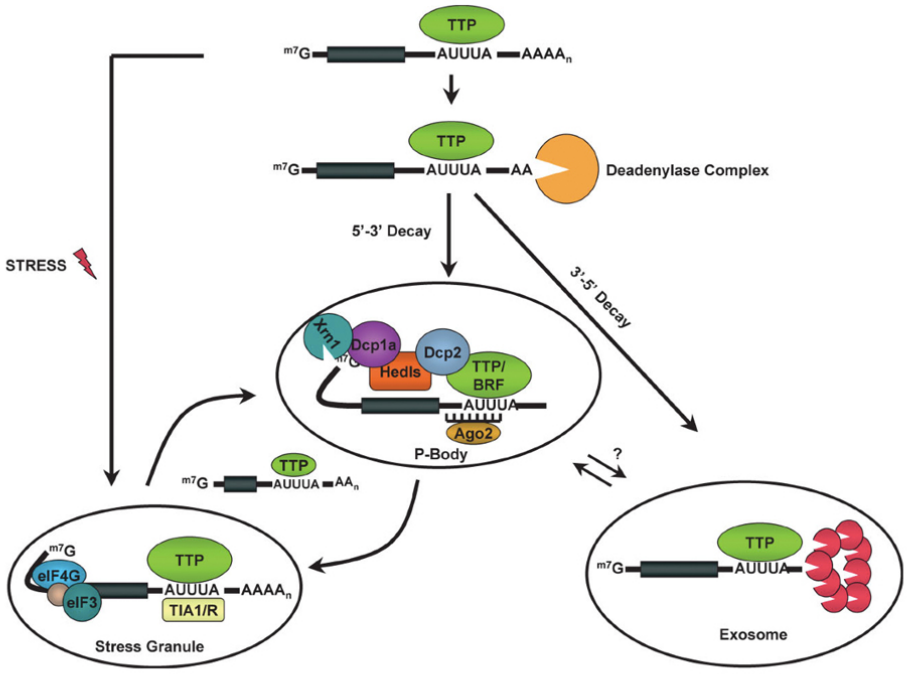

adapted from Sanduja, S., Blanco, F.F., and Dixon, D.A., Wiley Interdiscip Rev RNA (2011)

Fig.3 : ZFP36 (TTP) role in ARE-mediated mRNA decay. In the cytoplasm TTP associates to mature mRNA transcripts via ARE binding and recruits the deadenylase complex. The following step involves the 3'-5' exosome-mediated decay of target mRNAs, or alternatively, the 5'- 3' decay in P-bodies, where the transcript is decapped and the mRNA is stored or decayed by the exonuclease Xrn1. During cellular stress, TTP can be recruited to stress granules and may facilitate delivery of translationally-repressed ARE-containing mRNAs from stress granules to P-bodies for degradation.

Not surprisingly, ZFP36 has been involved in microRNA dependent post-transcriptional regulation, since it can interact with argonaute (Ago) proteins thus promoting mir-16 mediated decay of ARE-mRNAs (Jing et al., 2005). Along with the described cytosolic functions, ZFP36 can also modulate the stability of nascent RNAs in the nucleus, where it inhibits poly(A) tail synthesis by interacting with poly(A)-binding protein nuclear 1 as recently reported by (Su et al., 2012). To date, the decay kinetics of ARE-RNAs bound by RBPs are still not clear. Many reports show indeed that

ZFP36-dependent deadenylation and decay rates correlate with the binding affinities of ZFP36 to different types of ARE sequences, implying that the nucleotides surrounding the core ARE element 5'-AUUUA-3' influence the degradation of target mRNAs. To complete this last observation, it has also to be considered the role of other RNA-binding proteins that compete for ARE-binding, including the TIS11/TTP family members BRF-1 and BRF-2 and the stability factor HuR, which can influence ZFP36-mediated regulation of target mRNAs. All these findings led to the idea that the association of an ARE-mRNA with ZFP36 and the fate of the transcript depend on the integration of signals from multiple regulatory factors in a cell-specific manner (Al-Souhibani et al., 2010).

3.3 Post-translational regulation of ZFP36

In quiescent cells ZFP36 is mostly nuclear, while in response to growth factor stimulation rapidly moves into the cytoplasm (Taylor et al., 1995). The nuclear import of ZFP36 does not seem to depend on a nuclear localization signal (NLS) but it depends on the presence of the two zinc finger domains and is unrelated to the ARE-binding activity, suggesting that some amino acids of the zinc fingers are responsible for this activity (Phillips, 2002). The export into the cytoplasm is dependent on a leucine-rich amino-terminal nuclear export sequence (NES) and mutants with truncated NES are entirely nuclear (Phillips, 2002). It has been observed that ZFP36 is

highly phosphorylated in response to serum (Cao et al., 2006) and it is known that many serine and tyrosine residues on its amino acidic sequence are targets of upstream kinases such as ERK/MAPK, p38 MAPK, JNK, and PKB/AKT (Taylor et al., 1995; Cao et al., 2003; 2007; Mahtani et al., 2001). Phosphorylation of human ZFP36 on serine 60 and 186 by p38 MAPK/MK2 affects its localization in the cell by enhancing the interaction with 14-3-3 adaptor proteins in the cytoplasm (Johnson et al., 2002; Chrestensen et al., 2004). This interaction protects ZFP36 from the protein phosphatase 2A (PP2A) and promotes its stability (Sun et al., 2007).In vivo studies demonstrated that phosphorylated ZFP36 retains the ability to bind AU-rich elements on mRNAs but looses the efficacy in promoting mRNA decay probably due to its interaction with 14-3-3 adaptor proteins (Stoecklin et al., 2004; Sun et al., 2007). In vitro, it has been reported that phosphorylation of ZFP36 reduces its binding to AU-rich elements on messenger RNAs (Hitti et al., 2006). The contrasting observations from these experiments might be explained by the fact that AMD is a multi-step process that relies on the activity of many other factors than ZFP36 therefore it is plausible that phosphorylation affects ZFP36 ability to interact with other players of the AMD. In support of this a recent paper demonstrated that MK2 phosphorylation of ZFP36 inhibits the recruitment of the CAF1 deadenylase, blocking the ARE mediated mRNA decay (Marchese et al., 2010). Noteworthy, phosphorylation of ZFP36 by MK2 kinase had no effect on the ARE-binding activity of ZFP36 suggesting that interaction between ZFP36 and the deadenylase might be reduced as a result of by phosphorylation

(Marchese et al., 2010). Based on these observations, the current model for ZFP36 function hypothesizes that in response to an extracellular pro-inflammatory stimulus ZFP36 is rapidly induced and the phosphorylated and inactive form accumulates in the cell cytoplasm. As the stimulus ceases, phosphorylation-dependent repression of ZFP36 is relieved, leading to targeted decay of ARE-containing mRNAs expressed during inflammation (Fig.4).

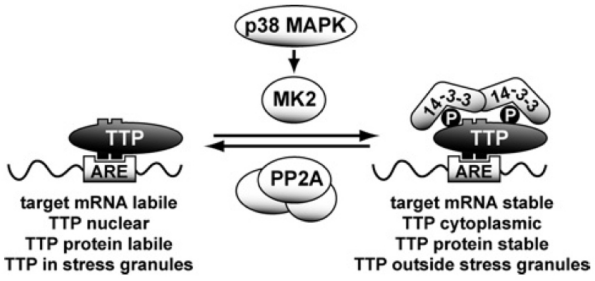

adapted from Sandler & Stoecklin, Biochem. Soc. Trans (2008)

Fig.4 : Post translational regulation of ZFP36 (TTP) by MK2 and PP2A. When unphosphorylated, TTP binds to the ARE-mRNAs and promotes AMD. Following phosphorylation by MK2, TTP assembles to the 14-3-3 adaptor proteins and ARE-mRNAs are stabilized. In this state, TTP is more stable and accumulates in the cytoplasm. The phosphatase PP2A dephosphorylates TTP causing its dissociation from the 14-3-3 adaptor proteins.

It has been recently reported that ZFP36 can be ubiquitinated by tumor necrosis factor receptor-associated factor 2 (TRAF2), with the effect of increasing ZFP36 stability (Schichl et al., 2011). This last finding reveals that other post-translational modifications that are different from phosphorylation regulates ZFP36, suggesting that still more has to be

discovered about ZFP36 function and regulation.

3.4 ZFP36 is a negative regulator of the inflammatory response

Molecular studies demonstrate that ZFP36 targets for degradation many ARE-carrying mRNAs that encode for pro-inflammatory cytokines (Tab 1) while *in vivo,* the confirmation that ZFP36 is a critical regulator of the inflammatory response came from ZFP36-deficient mice (Taylor et al., 1996).

Following targeted disruption of the Zfp36 gene, mice appear normal at birth, but within 1-8 weeks they develop a systemic autoimmune inflammatory syndrome characterized by cachexia, conjunctivitis, dermatitis, severe arthritis and alopecia (Taylor et al., 1996). Interestingly, this inflammatory phenotype is dependent upon complete loss of ZFP36, since heterozygous mice do not show chronic inflammation. Hematopoietic abnormalities including myeloid hyperplasia that results in enlarged spleen and lymph nodes, and thymic atrophy is another feature of the ZFP36 -/- mice. The knockout mouse model reveals that ZFP36 is an important physiological regulator of pro-inflammatory cytokines, moreover from literature data it seems that its altered expression might influence the onset and severity of inflammatory syndromes in humans. In particular, its role in the development of autoimmune pathologies has been investigated through the analysis of polymorphisms variation in healthy individuals and patients

with autoimmune diseases. The study from Carrick and colleagues associated the single nucleotide polymorphism (SNP) ZFP36*8, a C to T transition in exon 2 with a higher incidence of rheumatoid arthritis (RA) in African-American individuals. Prediction studies reveal that the presence of this SNP cannot alter the folding or the activity of ZFP36, suggesting that it can impact on the transcription or translation of ZFP36 mRNA (Carrick et al., 2006).

Tab.1

Cellular Process	mRNA Target
Inflammation and Cancer	Ccl2
	Ccl3
	CD86
	c-fos
	cIAP2
	c-myc
	COX-2
	DUSP1
	E6-AP
	E47
	GM-CSF
	IDC
	Interleukins (IL-2, IL-3, IL-6, IL-10, IL-12)
	IFN-gamma
	iNOS
	LATS2
	MHC (Class 1B and F)
	MMP-1
	PAI-2
	SOD2
	TNF-alpha
	TTP
	uPA
	uPAR
	VEGF
Cell Cycle	Cyclin D1
	MIP-2
	p21
	Plk3
Other	1,4-galactosyltransferase
	Ier3
	PITX2

adapted from Sanduja S., Front Biosci (2012)

NF-kB signaling cascade plays a major role in mediating the inflammatory stimuli driven by TNF-alpha (Hsu et al., 1995) and ZFP36 can modulate this pathway by targeting TNF-alpha mRNA for degradation (Lai et al., 1999).Recent studies revealed a more complex function for ZFP36 in inhibiting NF-kB signaling. Schichl and colleagues demonstrated that ZFP36 counteracts NF-kB activity by interfering with the nuclear translocation of the p65/RelA subunit of NF-kB (Schichl et al., 2009). The same group recently reported that the phosphorylated form ZFP36 favors JNK signaling against NF-kB upon TNF-alpha receptor engagement (Schichl et al., 2011). Another study showed a physical interaction between ZFP36 and the histone deacetylases (HDACs), HDAC-1, HDAC-3, and HDAC-7, thereby functioning as a co-repressor for NF-kB-dependent transcription (Liang et al., 2009a).

3.5 Role of ZFP36 in cancer

A nascent field of research associates loss of ZFP36 expression with cancer and it has been demonstrated that re-expression of ZFP36 in human and murine tumor models has an anti-growth effect, making ZFP36 a candidate tumor suppressor gene (Stoecklin et al., 2003; Zanocco-Marani, 2010). This hypothesis is strengthened by the fact that many ARE-mRNAs encode for oncogenes (Tab.1) up-regulated during cancer progression (Fig.5). On the other hand, it is believed that chronic inflammatory status might predispose

to an increased risk of malignant transformation (Pikarsky et al., 2004; Khabar, 2010), therefore loss of ZFP36 expression might correlate with an increased chance of cancer development (Carrick and Blackshear, 2007; Brennan et al., 2009).

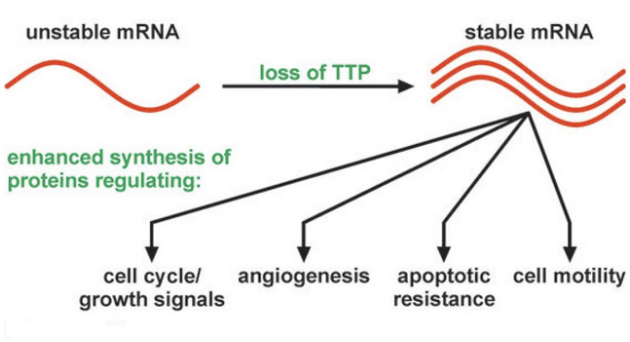

adapted from Brennan, S.E. et al.,Cancer Res (2009)

Fig. 5: Loss of ZFP36 (TTP) expression leads to the stabilization of mRNAs coding for oncogenes. Many ARE-carrying mRNAs encode for genes involved in growth factor response, angiogenesis, apoptotic resistance and cell motility. It is believed that loss of ZFP36 expression might favor the stabilization of this group of mRNAs, leading to an enhanced synthesis of proteins involved in key oncogenic pathways.

A recent paper from Rounbehler and colleagues confirms the idea that ZFP36 is a tumor suppressor gene and that its loss is associated with tumor development. They show in precancerous and Myc-overexpressing B cells, that Myc actively down-modulates the expression of ZFP36, resulting in a critical de-regulation of hundreds of ARE-carrying mRNAs and restoring ZFP36 impairs Myc-induced lymphomagenesis and abolishes maintenance of the malignant state. Further, they show that there is a selection for ZFP36 loss in malignancy thus confirming its function as a tumor suppressor (Rounbehler et al., 2012). Interestingly a previous work from Marderosian and colleagues showed that Myc's mRNA is a target of degradation by ZFP36 (Marderosian et al., 2006) and under the light of recent discovery, these two reports unveil how Myc oncogene must silence ZFP36 tumor

suppressor in order to safeguard its own stability and promote cancer progression. Earlier interesting reports evidenced that ZFP36 attenuates the malignant phenotype also in tumors not characterized by Myc overexpression and outside the hematopoietic context, which is not surprising if we consider that ZFP36 might target for degradation a long list of oncogenes, growth factor and pro-inflammatory cytokines with a critical role in the homeostasis of the majority of human tissues. Stoecklin and colleagues showed that overexpression of ZFP36 in a v-H-ras-dependent mast cell tumor mouse model delays tumor progression (Stoecklin et al., 2003). Recently, it was reported that ZFP36 expression levels are inversely correlated with aggressiveness, metastatic potential, and resistance to anti-tumorigenic treatment in breast cancer (Brennan et al., 2009; Gebeshuber et al., 2009; Al-Souhibani et al., 2010). Many works show that cervical cancer-derived tissues and cell lines display a loss of ZFP36 expression, suggesting that ZFP36 may be an important player in the pathology. Consistent with this, TTP re-expression in HPV18-transformed cervical cancer cells led to inhibition of cellular proliferation (Sanduja et al., 2009). As regards colon cancer, a recent work from the same group has shown that loss-of-ZFP36 and gain-of-HuR functions in colon cancer are required to promote expression of COX-2 and ectopic expression of ZFP36 attenuates cell proliferation, and inhibits COX-2 expression (Young et al., 2009). In liver, a comparison between normal tissue and hepatocellular carcinoma (HCC) cell lines shows a significant down-regulation of ZFP36 (Sohn et al., 2010) due to the hypermethylation of a CpG island in the Smad biding site

on ZFP36 promoter. Treatment with 5-aza-deoxycytidine made possible to restore ZFP36 expression in response to TGF-b and up-regulation of ZFP36 correlated with down-regulation of Myc and growth inhibition.

3.6 Hypothesizing the therapeutic exploitation of ZFP36

As mentioned above, ZFP36 is involved in a set of physiological process were its loss can promote inflammation and possibly predispose to cancer. Based on the fact that numerous ARE-containing mRNA encode for genes involved in carcinogenesis, tumoral angiogenesis (Khabar, 2005) and inflammation, it is conceivable that prolonged re-expression of ZFP36 in tumor cells could represent a valid therapeutic option aimed at targeting multiple pathways in cancer and inflammatory syndromes. Currently, our lab is conducting a study to evaluate the therapeutic effect of a cinnamon-derived polyphenolic compound that we shown to induce ZFP36 and ZFP36L1 expression in human hematopoietic stem cells (Vignudelli et al., 2010) The rationale of this approach arises from the fact that TIS11 proteins target for degradation STAT5b, which is an up-regulated mediator of EPO signaling in the Policitemia Vera class of hematological malignancies (Prchal et al., 1978; Spivak, 2002). We demonstrated that TIS11-mediated down-regulation of STAT5b following polyphenolic treatment can interfere with erythroid differentiation of hematopoietic stem cells (Vignudelli et al., 2010) and our goal is now to validate this mechanism in Policitemia Vera

stem cells collected from patients. To date, approaches aimed at ZFP36 restoration with a therapeutic goal are missing, but still due to their ability to interfere with multiple pathways, ZFP36 and the TIS11 family look very promising anti-inflammatory and anti-cancer agents.

4. MALIGNANT GLIOMAS

4.1 Glioblastoma

Gliomas arise from the "gluey," or supportive tissue of the brain. There are several different types of gliomas. The type of glioma is determined by the cells that give rise to the tumor. Astrocytoma, oligodendroglioma, glioblastoma, oligoastrocytoma are all examples of gliomas. Glioblastoma multiforme (GBM) is the most common and malignant subset of brain tumors, classified as grade IV astrocytoma by the World Health Organisation (WHO) (Maher et al., 2001). GBM have been profiled at the molecular level leading to a differentiation of GBM in different subclasses of the disease (Mischel et al., 2003; Louis, 2006; Phillips et al., 2006). However, each tumor contains variable proportions of differentiated cell types and anaplastic cells, which complicates accurate diagnosis and grading. Despite the success in identifying the deregulated signaling pathways and the characteristic genetic defects associated with gliomas

(Furnari et al., 2007) (Cancer Genome Atlas Research Network, 2008), it remains unclear how these operate in the different subsets of cells that compose these heterogeneous tumors. Standard first line treatment for glioblastoma patients includes surgery followed by focal fractionated radiotherapy with concomitant and adjuvant administration of the alkylating chemotherapy, temozolomide. The addition of temozolomide significantly improves the median, 2- and 5-year survival compared to radiotherapy alone in patients with newly diagnosed glioblastoma. Nevertheless, glioblastoma patients have a poor prognosis with a median survival of 14.6 months. A recognized predictor for tumor response to temozolomide is the epigenetic silencing of the O6-methylguanine-DNA-methyltransferase (MGMT) gene promoter by methylation (Weller et al., 2010). The ubiquitous DNA repair protein MGMT counteracts chemotherapy-induced DNA damage by restoring the structural integrity of O6-alkylated bases. Around half of all GBM patients harbor an un-methylated MGMT promoter, and these seem to respond poorly to temozolomide chemotherapy. To date there is no alternative treatment for this group. Thus, understanding the mechanisms mediating cellular survival and apoptosis resistance will enable to exploit the key players to design smarter drug combinations in targeted cancer therapies. GBMs have been traditionally defined as two clinically and cytogenetically distinct diseases, the primary or de novo vs the secondary GBMs. The latter classically afflict younger persons (median age ~45 years) and evolve from the slow progression (mean, 4-5 years) of a low-grade glioma, which usually displays aberrations in platelet derived growth factor

receptor (PDGFR) and TP53 genes. Primary GBMs present acutely (with a clinical history less than 6 months) as a high-grade disease that most frequently affects the elderly (median age ~60 years). They typically harbor mutations in epidermal growth factor receptor (EGFR), cyclin-dependent kinase inhibitor 2A (CDKN2A) and loss of heterozygosity (LOH) on chromosome 10q23, which houses the phosphatase and tensin homolog (PTEN) gene. LOH on chromosome 10 is the most frequent genetic alteration in primary GBMs, occurring in 60-80% of cases (Krakstad and Chekenya, 2010). Mutations in the EGF receptor result in ligand independent constitutive tyrosine kinase activity that activates persistent downstream RAS/RAF/MAPK growth and PI3K survival signaling (Frederick et al., 2000). As regards the invasion potential of glioblastomas, extensive studies show that STAT3 (through JAK/Stat pathway) and NF-kB transcription factors support migratory and invasive potential of glioblastoma cells (Senft et al., 2010; Raychaudhuri and Vogelbaum, 2011). In particular, constitutive NF-kB activity positively regulates the expression of VEGF and IL-8 and tumor angiogenesis of human glioblastoma (Xie et al., 2010). Although much is known about the diverse genotypes causing the heterogeneous histological phenotypes of GBMs and how they impact on survival signaling, there is still no therapy that induces tumor cell apoptosis beyond that of the standard treatment. Several studies on GBM clearly demonstrate, that targeting of IAPs (Inhibitor of apoptosis proteins) sensitizes cells to apoptosis (Ziegler et al., 2008) and a recent report showed that XIAP inhibitors synergizes with radiation to increase

glioblastoma cell apoptosis (Vellanki et al., 2009). Furthermore, targeting of IAPs also increases sensitivity to TRAIL induced apoptosis (Siegelin et al., 2009). Interestingly, several players in the GBM tumor paradigm, such as VEGF, IL-8, NF-KB, and STAT5b, have already been described as direct targets of TIS11 genes, while others, as STAT3, PIM1, PIM3 and XIAP can be considered putative ones since they carry AU-rich elements in their mRNAs' 3'-UTR. This observation suggests that, by acting on the expression of TIS11 genes, it might be possible to impinge on GBM growth, viability and chemoresistance by determining the down-regulation of several oncogenes.

4.2 Oligodendroglioma

Oligodendroglioma is a subclass of gliomas that accounts for 5-18% of all cases and it has been shown that 60-90% of these tumors are characterized by the concomitant loss of a single copy of chromosomes 1p and 19q (Reifenberger et al., 1994; Smith et al., 1999) Interestingly, the ZFP36 gene locus is located on 19q and published data shows that its expression is down-regulated in a high number of patients derived samples, as shown by expression data taken from Sun et al., (Sun et al., 2006) (Fig.6). The 1p/19q loss is a signature that strongly correlates with survival and response to therapy but still, despite the fact that 1p/19q deletion analysis is monitored in the diagnosis and treatment of oligodendrogliomas,

the presumed tumor suppressors resident in these genomic loci (1p, 19q) remain elusive (Huse and Holland, 2010).

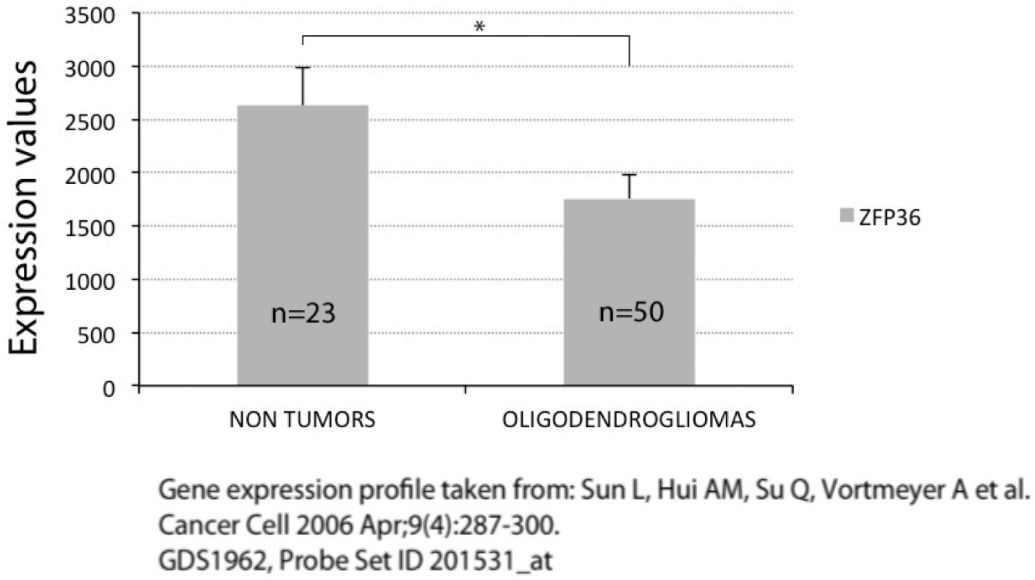

Fig.6 : ZFP36 expression in non tumor samples vs Oligodendrogliomas. Analisys of gene expression profiles from Gene Expression Omnibus (GEO) Data Sets (http://www.ncbi.nlm.nih.gov/gds) reveals a down-regulation of ZFP36 expression in oligodendroglioma-derived samples when compared to non-tumor specimens.

4.3 Glioma-derived cancer stem cells

Within established Gliomas, a subpopulation of cancer cells with stem-like properties (Glioma stem cells, GSCs) has been proposed to contribute to resistance to therapy and disease progression (Singh et al., 2004; Bao et al., 2006; Piccirillo et al., 2006; Pollard et al., 2009; Mannino and Chalmers, 2011). Gliomas are very heterogenic diseases and the GSCs are considered the major determinant of the heterogeneity that can be characterizes each

Glioma (reviewed in Venere et al., 2011). Self-renewal in normal and tumor stem cells occurs when a cell divides to produce a daughter cell with the same developmental potential (He et al., 2009a). Normal adult neural stem cells have been identified in the sub-ventricular zone (SVZ); they represent a rare, slow-cycling and self-renewing population that give rise to more rapid cycling transit amplifying cells, which then give rise to more differentiated neuroblasts (Doetsch et al., 1997). GSCs are similar to the neural adult stem cells population and are defined by their capacity to (1) self- renew *in vitro*, (2) initiate tumor formation following xenotransplantation, and (3) generate tumors that recapitulate the heterogeneity of the parental tumors (Stiles and Rowitch, 2008). Based on the cancer stem cells hypothesis (Reya et al., 2001), this population of stem cells would underlie a cellular hierarchy and drive tumor growth through sustained self-renewal and would be the hypothetical ideal target for anti tumor therapy. To date, putative cancer stem cells have been isolated from diverse adult and childhood brain tumors using the neural stem cell marker Prominin (CD133) (Hemmati et al., 2003; Singh et al., 2003) and these can initiate tumor formation following xenotransplantation (Singh et al., 2004). Long-term expansion of GSCs has been achieved both in the form of neurospheres culture (Galli et al., 2004) and adherent culture (Scheffler et al., 2005; Pollard et al., 2009).

The GSCs represent a powerful model to investigate cellular and molecular mechanisms underlying self-renewal, differentiation and tumor formation, which are underscored when addressed using common cell lines.

Nevertheless, caution has to be taken in he exploitation of this model; in fact many divergent results on GSCs can be found in literature. For example, the degree to which glioma stem cells resemble neural stem cells, and the degree to which the normal lineage hierarchy is maintained in brain tumors remain unanswered questions. Moreover, many studies have shown that both CD133+ and CD133- cells can self-renew and generate tumors, for a review see ref (Barrett et al., 2012), rising questions about the specificity of CD133 as a specific marker of GSCs. A recent report also showed that self-renewal ability of GSCs does not predict tumor growth potential in mouse models of high-grade Glioma (Barrett et al., 2012).

Due to the high heterogeneity of gliomas, further studies are required to define the role of GSCs in the different subtypes of this tumor in order to identify the optimal cell populations for therapeutic targeting.

5. NECROPTOSIS

Programmed cell death is a mechanism by which harmful cells dye during development, in homeostasis or in pathogenic conditions and this mechanism is often deregulated in tumors (Hanahan and Weinberg, 2011). Apoptosis and necrosis are considered the two main forms of cell death, and in particular apoptosis has been regarded as the programmed form of cell death while necrosis was thought to happen accidently. Despite necrosis has been considered for long time an uncontrolled form of cell

death, evidence is accumulating that the execution of necrotic cell death may be finely regulated by a set of signal transduction pathways and catabolic mechanisms (Galluzzi and Kroemer, 2008; Berghe et al., 2009) For this reason it has been recently adopted the term "necroptosis" to indicate regulated necrosis. *In vitro*, necrosis is morphologically characterized by rounding of the cell, cytoplasmic swelling, presence of dilated organelles and absence of chromatin condensation (Festjens et al., 2006; Degterev and Yuan, 2008). The hypothesis that necrosis is a regulated form of cell death came initially from the finding that TNF-alpha could trigger both apoptotic and necrotic cell death (Laster et al., 1988) and in particular, necrosis was triggered by TNF in the absence or by inhibition of the initiator Caspase (Caspase8) (Lemaire et al., 1998; Vercammen et al., 1998). Other studies revealed that TNF, TNF-related apoptosis-inducing ligand (TRAIL) and CD95L (FASL) are able to trigger caspase-independent necroptotic cell death in T cells and that this effect relies on the death domain-containing Receptor-interacting serine/threonine- protein kinase 1 (RIPK1/RIP1) (Holler et al., 2000; Vanlangenakker et al., 2012). The critical role of RIP1 in the execution of necroptosis became clear after the discovery that necrostatin 1 (NEC1), a specific inhibitor of RIP1 kinase activity, could completely inhibit necroptosis both *in vitro* and *in vivo* (Degterev et al., 2005; 2008). Further studies revealed that another member of the RIP family, named RIP3, has a critical role in this process, specifically in antigen-stimulated T cells lacking catalytically active caspase-8 (Cho et al., 2009; He et al., 2009b; Lu et al., 2011). In vivo experiments helped to elucidate the molecular basis of

necroptosis and the relationship with apoptosis. Knock out mice for most of the pro-apoptotic capases showed in an increase in cell numbers, due to the loss of the ability to execute programmed cell death. However, deletion of pro-apoptotic caspase 8, FAS-associated death domain protein (FADD) (that specifically interacts with caspase 8) or the caspase 8 inhibitor, FLICE inhibitory protein (FLIP), all lead to embryonic death at day 10.5, suggesting that caspase 8, FADD and FLIP might be involved in an alternative from of cell death to apoptosis. Intriguingly, the concurrent deletion of pro-apoptotic and pro- necrotic molecules, such as the double deletion of caspase 8 and RIP3 or FADD and RIP1, rescues the embryonic lethality (reviewed in Peter Kreuzaler and Christine J. Watson 2012 (Kreuzaler and Watson, 2012). The death inducing complex II, which assembles in the cytoplasm after activation of the TNF receptor signaling, has been regarded as the place where the death decisions takes place (Micheau and Tschopp, 2003). In the complex II, caspase 8 homodimers become active after auto-protolytic cleavage and the result of this process is the induction of apoptosis. However, FLIP can bind to caspase 8, preventing its dimerization and activation, thus interfering with the onset of the apoptotic program (Krueger et al., 2001). In this complex, a complete inactivation of caspase 8 has been shown to lead to a concomitant activation of RIP1 and the induction of necroptosis (Oberst et al., 2011). All these findings suggest that cells sense different intracellular and extracellular death signals and respond by assembling a death-inducing complex composed of pro-apoptotic and pro-necrotic molecules. In case this

complex fails in the execution of the apoptotic program (e.g. inhibition of caspase8, deletion of FADD adaptor protein), the default response is necroptosis that relies on the kinase activity of the key enzymes RIP1 and RIP3 (Fig.7).

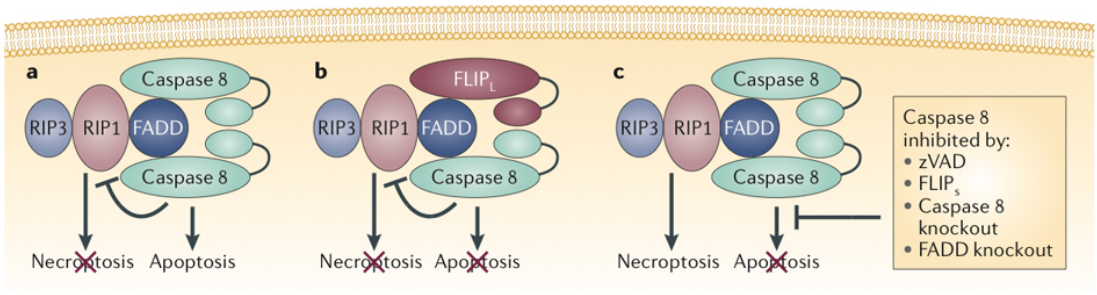

adapted from Kreuzaler P. & Watson C.J., Nat Rev Cancer (2012)

Fig.7 : The interplay between caspase 8 and RIP1 activity determines the outcome of many death stimuli. A. Dimerization of caspase 8 in complexes such as complex II leads to the full activation of caspase 8 and the induction of apoptosis. In this setting RIP1 is inhibited by caspase 8, thus preventing the initiation the necroptotic program. **B.** The heterodimer formed by caspase 8 and FLIPL results in an attenuated caspase 8 activity that determines a block of apoptosis but still inhibits RIP1, thus leading to cell survival. **C.** Different stimuli can inhibit caspase 8 leading to a stabilization of RIP1 and execution of necroptotic cell death.

Phosphorylation of RIP1 at Ser 161 and RIP3 at Ser 199 occur after necrotic stimuli, and these phosphorylations are considered essential for necroptosis to proceed (He et al., 2009b). Necroptosis is characterized by important metabolic changes that take place following RIP1 and RIP3 activation, among these it has been described an increase in the glycolytic rate concomitant with an excess of energy consumption, thus leading to a critical decline in ATP availability and cleavage Poly [ADP-ribose] polymerase 1 (PARP), all followed by lysosomal membrane permeabilization (Vandenabeele et al., 2010). Despite our knowledge of many metabolic and

molecular aspects of necroptosis, the targets of RIP1 and RIP3 kinases are still uncharacterized and it is unclear whether other kinases are involved in the execution of necroptosis. To date, the biochemical method used to discriminate necroptosis from other forms of cell death is the inhibition of RIP1 activity through the drug NEC1 (Vanlangenakker et al., 2012).

5.1 The ripoptosome

Two recent studies unveiled the existence of a signaling platform that integrates various stress inputs into a potent death message, resulting in cell death with either apoptotic or necrotic features (Feoktistova et al., 2011; Tenev et al., 2011). In response to cellular stress, such as DNA damage following exposure to the topoisomerase II inhibitor etoposide, RIP1 recruits FADD and caspase 8 to form a 2 Mega Dalton complex called Ripoptosome. This complex is distinct and its assembly is independent from the complex II downstream of TNFR (Micheau and Tschopp, 2003; Feoktistova et al., 2011; Tenev et al., 2011), nevertheless both can trigger cell death via necroptosis. Both the death complexes require the activity of RIP1 to execute death and share some components, therefore the inhibition of RIP1 by its specific inhibitor NEC1 acts on both the death inducing platforms. It has been suggested that the Ripoptosome is inhibited by FLIPL while its activity is promoted by FLIPS, a shorter splice variant of FLIPL (Feoktistova et al., 2011). Another mechanism that specifically leads to

Ripoptosome inactivation is the ubiquitination of RIP1 by inhibitor of apoptosis proteins, specifically by c-IAP1 (BIRC2) c-IAP-2 (BIRC3) and XIAP (BIRC4) (Feoktistova et al., 2011; Tenev et al., 2011). It is believed that IAP proteins ubiquitinate RIP1 to promote its degradation by the proteasome (Bertrand et al., 2008; Darding et al., 2011), leading to the disassembly of the Ripoptosome. This molecular finding is supported by the fact that concomitant inhibition of at least two of the IAPs proteins is sufficient to promote the RIP1 stability and Ripoptosome assembly (Tenev et al., 2011). Importantly, to date, Ripoptosome formation has been reported to happen only in response to etoposide treatment, therefore the physiological inducers of the formation of this complex are still missing to our knowledge. IAPs in turn could be inhibited by the second mitochondria-derived activator of caspases (SMAC) that is released from mitochondria during apoptosis (Du et al., 2000). Small-molecule mimetics of SMAC have been developed and have been shown to be highly efficacious in down-regulating IAPs (Vince et al., 2007). In fact, the formation of the ripoptosome has been achieved by using SMAC mimetics, or by inducing heavy cellular stress through etoposide, which resulted in IAPs down-regulation (Darding et al., 2011) (Fig.8). Importantly, Ripoptosome formation in response to cellular stress or to inhibition of IAPs does not occur in non-cancerous cells, presumably because cancer cells frequently have higher levels of both RIP1 and caspase 8 (Tenev et al., 2011).

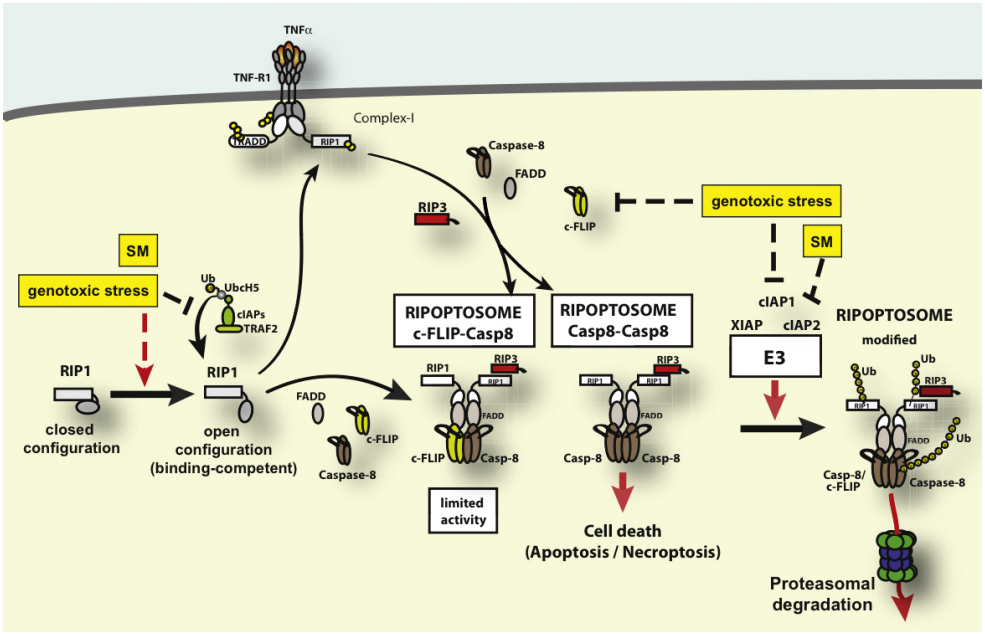

adapted from Tenev T., Bianchi K., et al, Molecular Cell (2011)

Fig.8 : Genotoxic damage and depletion of IAPs result in Ripoptosome formation. In normal conditions RIP1 is in closed configuration and only a small percentage of RIP1 is targeted for ubiquitination by IAPs (c-IAP1, c-IAP2 and XIAP). In response to genotoxic stress or smac mimetics treatment (SM) IAPs are down-modulated and RIP1 is derepressed and binds to FADD. Ripoptosome assembly stimulates caspase-8 activation and/or necroptosis, depending on cellular context. Importantly, the Ripoptosome can form independently of death ligands or mitochondrial pathways. Ripoptosome assembly stimulates caspase-8 activation and/or necroptosis, depending on cellular context. (for a complete review see Tenev 2009).

6. X-LINKED INHIBITOR OF APOPTOSIS XIAP

The X chromosome-linked inhibitor of apoptosis, XIAP (BIRC4), is a key regulator of apoptosis, due to its ability to bind to and inhibit both initiator and effector caspases (Holcik and Korneluk, 2001). Overexpression of XIAP is seen in a number of human cancers, including glioblastoma and as mentioned before, loss of XIAP was shown to sensitize glioblastoma cell lines to cell death (Ziegler et al., 2008) and to correlate with enhanced chemo or radiation resistance (Holcik et al., 2000; Tamm et al., 2000; Gyrd-Hansen and Meier, 2010).

XIAP contains two types of conserved sequence motifs, the baculovirus IAP repeats (BIRs) and the zinc finger-like RING finger. Three BIR repeats have the ability to bind to capases, in particular the second BIR associates with caspases 3 and 7 (Takahashi et al., 1998; Sun et al., 1999; 2000) while the third BIR binds caspase 9 and are necessary for XIAP to inhibit caspase activity. Although the presence of a BIR is often considered as the defining feature of IAPs, XIAP contains a second class of domain, which is also found in other c-IAPs (c-IAP1, c-IAP2), a C3HC4 RING finger motif 13, that functions as an E3 ubiquitine ligase involved in the proteasome pathway and that has been shown to target RIP1 and SMAC for degradation (Duckett, 2009; Darding and Meier, 2012) The RING finger is situated at the carboxyl terminus of the protein. XIAP is encoded by two distinct mRNAs that differ in their 5′ UTRs: the short 5′ UTR promotes the basal level of XIAP expression under normal growth conditions. The less abundant, longer 5′

UTR (1.7-kb-long) contains a 162-nt Internal Ribosome Entry Site (IRES) element that allows favors the translation of XIAP mRNA during cellular stress and apoptosis (Riley et al., 2010). Interestingly, XIAP harbors an ARE sequence in its 3' UTR therefore mRNA degradation by the AMD mechanism might counteract the activity of the IRES leading to a down-regulation of XIAP even during cellular stress. This last finding supports the idea that ZFP36 might promote the down-regulation of XIAP's mRNA, thus interfering with the resistance to apotosis of cells over-expressing XIAP.

7. PROMIELOCYTIC INTEGRATION SITE FOR MOLONEY KINASES (PIM KINASES)

The "promielocytic integration site for Moloney" (PIM) proteins are a family of short-lived serine/threonine kinases that are highly conserved in multicellular organisms. This kinase family comprises three members named PIM1, PIM2 and PIM3 all regulated by the Ca2+/Calmodulin complex (Nawijn et al., 2011). These kinases are highly homologous between them, especially PIM1 and PIM3 show 71% identity at the protein level and this results in the functional redundancy for all the three kinases (Mikkers et al., 2004; Mukaida et al., 2011). Pim1 gene is transcribed in two distinct mRNA isoforms, Pim2 codes for three different mRNAs, while only one transcript

has been described for Pim3 so far, but all the PIM isoforms maintain the serine/threonine kinase activity in vitro (Xie et al., 2006). Noteworthy, Pim1, Pim2 and Pim3 mRNAs carry ARE sequences in their 3'UTR and this would account for the short life of these messengers in physiological conditions (Mikkers et al., 2004). Nevertheless, to date none of the known ARE binding proteins have been described in complex with Pim mRNAs, making the post-transcriptional regulation of their stability an open question. As regards post-translational regulation, all PIM kinases are constitutively active when expressed, meaning that their regulation takes place at the transcriptional start sites, at the mRNA level (Lilly et al., 1999), or by protein stabilization (Amaravadi and Thompson, 2005; Nawijn et al., 2011). PIM kinases are ubiquitously expressed with an enrichment of PIM1 in the hematopoietic tissue, PIM2 in lymphoid and brain cells and PIM3 in the brain and breast contexts (Blanco-Aparicio and Carnero, 2012). The induction of the expression of this family of kinases is mainly driven by the JAK/STAT pathway in response to ligand binding on cytokines membrane receptors (Blanco-Aparicio and Carnero, 2012). In cancer, PIM kinases are found overexpressed in tumors both of hematological and epithelial origin. PIM1 overexpression in tumor specimens is not due to re-arrangements or amplification of the coding gene, instead, its expression probably results from sustained transcriptional activity driven by the NF-kB transcription factor. In diffuse large B cell lymphoma, follicular lymphoma, Hodgkin's and mucosa- associated lymphoid tissue-type lymphoma, aberrant somatic hypermutation of PIM1 has also been observed. Recent reports indicate the

PIM kinases as strong promoter of cellular migration and tumor invasion in a model of prostate cancer (Santio et al., 2010). Usually PIM kinases exert their oncogenic activity in cancers characterized by the overexpression of MYC and it has been demonstrated, at least for PIM1, its active cooperation with MYC in regulating gene expression at the promoter level. Other oncogenic activities of these kinases are the promotion of both cell cycle progression and survival signaling through phosphorylation of BAD (Aho et al., 2004).

8. MATERIALS AND METHODS

8.1 Cell cultures and treatments

The human glioma cell line ln827 was cultured in DMEM medium (Euroclone) supplemented with 10% heat-inactivated fetal bovine serum (Biowhittaker), 2 mM L-glutamine and penicillin/streptomycin (100 µg/ ml) (Euroclone). Human GSCs and all clones were cultured as describe (Pollard 2009) Briefly, cultured flasks were coated with Laminin (Sigma) for 3 h at 10 mg/ml before to use. GSCs were routinely grown at confluence and then dissociated using Accutase (Sigma). Neurocult NS-A media (stem Cell Technologies, Grenoble, France) is supplemented with the GFs EGF and FGF-2. GP + envAm12 cells and Phoenix Ecotropic packaging cells were obtained from ATCC and cultured respectively in DMEM medium (Euroclone) or IMDM supplemented with 10% heat-inactivated fetal bovine serum (Biowhittaker), 1 mM L-glutamine and penicillin/streptomycin (100 µg/ml) (Euroclone). Human embryonic kidney HEK293T cells were cultured as above in a 5% CO2-humidified atmosphere at 37 °C. Cinnamon polyphenol extracts were solubilized in DMSO, then added to complete culture medium at the final concentration of 0.01, 0.1, or 0.25 µg/µl. The medium was not changed until cells were lysed for RNA/protein collection or colonies were scored.

8.2 Plasmids and retroviral vectors

Full-length ZFP36 was generated by RT-PCR performed on total RNA extracted from U937 cells using ZFP36-direct primer (DP) (5'-ATGGATCTGACTGCCATCTACG-3') and ZFP36-reverse primer (RP) (5'-CGGGCAGTCACTTTGTCACT-3') for U937 cell line culture conditions refer to Vignudelli et al., 2010. Amplification was carried out using Fast Start High Fidelity PCR System (Roche Applied Science), and the amplified fragments were inserted into the pCR 2.1-TOPO T/A cloning vector (Invitrogen) where they were fully sequenced to exclude polymerase- induced mutations.

ZFP36 cDNA was then EcoRI digested and subsequently cloned within the EcoRI ends of pBABE puro retroviral vector or of pcDNA3.1 expression construct, resulting, respectively, in pBABE ZFP36 and pcDNA3.1 ZFP36 constructs. FlagZFP36 fragment was RT-PCR amplified using FlagZFP36-Direct Primer (DP) (5'-ATG GAC TAC AAA GAT GAC GAC GAC AAG GAT CTG ACT GCC ATC TAC-3') and ZFP36-Reverse Primer (RP) (5'-CGG GCA GTC ACT TTG TCA CT-3'), and the amplified fragments were inserted into the pCR2.1-TOPO T/A cloning vector, from which they were EcoRI excised and cloned into an EcoRI-digested pcDNA3.1 vector. PIM1, PIM3 and XIAP ARE-containing 3' UTR were amplified by RT-PCR on total RNA extracted from ln827 cells using PIM1 3' UTR-DP (5'-ATG CGC ATT CTA ACC TGG AG-3') and PIM1 3'UTR RP (5'-GAT CTC TTT TAT TCC CCT GTA CAG TAT TT-3'), PIM3 3' UTR-DP (5' GCA CAC ACA ATG CAA GTC CT-3') and PIM3 3' UTR RP (5'-ACT GAA AGA ACC CCC ATC TG-3'), XIAP 3'UTR DP (5'-TTC ATA GAA

CGT CCA GGG TTT A-3') and XIAP 3' UTR RP (5'- GAA GCT GAG GCA CGA GAA TC-3'). The amplified fragments were then inserted into the pCR2.1-TOPO T/A cloning vector and were fully sequenced. The 3' UTR fragments were then EcoRI excised, blunted and cloned in the sense orientation into a SmaI-digested pGL3-Promoter Vector (Promega) that had previously been modified in order to transfer the multiple cloning region downstream the luciferase reporter gene. DNA transfection and retroviral infection. Transient transfection of pcDNA3.1-based constructs was performed using Fugene HD reagent (Roche Applied Science) as suggested by the manufacturer's guidelines. The ln827 cell line was transduced using pBABE empty control vector or pBABE ZFP36 retroviral vector. Packaging lines for the pBABE-based constructs were generated by transinfection in the ecotropic Phoenix and successive infection of amphotropic GP + envAm12 cells. Stable packaging cell lines were then produced by 1 µg/ml puromycin selection. Ln827 were transduced by two cycles of infection (6 h each) with viral supernatant in the presence of polybrene (8 µg/ml). Transduced ln827 were selected by mean of one cycle of 0.5 µg/ ml puromycin treatment.

8.3 Oligonucleotide-mediated gene silencing

Ln827 cells were treated with Lipofectamine RNAiMAX (Invitrogen) reagent and transfected with a mix of three predesigned siRNAs as per the manufacturer's instructions. PIM1 siRNAs (Hs01_00073783, Hs01_00073785,

Hs01_00073786, Sigma Aldrich); PIM3 siRNAs (Hs01_00152603, Hs01_00152604, Hs01_00152605, Sigma Aldrich); XIAP siRNAs (Hs02_00331284, Hs02_00175694, Hs02_00175695, Sigma Aldrich) or control siRNA (Sigma Aldrich SIC001). After 18 h, the medium was replaced with complete DMEM medium. Cells were processed 72 h after transfection. RT-PCR and real-time PCR. Total cellular RNA was extracted using the EuroGOLD Total RNA kit (Euroclone) or RNeasy MicroKit (Qiagen). RNA integrity and concentration was then assessed by the Bio-Analyzer technique (Applied Biosystems). For RT-PCR, 3 µg of total RNA were reverse transcribed using M-MLV reverse transcriptase (Invitrogen), and then expression of specific genes was assessed by PCR amplification performed using specific primers: GAPDH-DP (5'-GAA GGT GAA GGT CGG AGT C-3'), GAPDH-RP (5'-GAA GGC CAT GCC AGT GAG CT-3'); ZFP36 DP (5'-ATG GAT CTG ACT GCC ATC TAC-3') ZFP36 RP (5'-CGG GCA GTC ACT TTG TCA CT-3'); PIM1 3' UTR-DP (5'-ATG CGC ATT CTA ACC TGG AG-3') and PIM1 3' UTR RP (5'-GAT CTC TTT TAT TCC CCT GTA CAG TAT TT-3'), PIM3 3' UTR-DP (5'-GCA CAC ACA ATG CAA GTC CT-3') and PIM3 3' UTR RP (5'-ACTGAAAGAACCCCCATCTG-3'), XIAP 3' UTR DP (5'-TTC ATA GAA CGT CCA GGG TTT A-3') and XIAP 3' UTR RP (5'-GAA GCT GAG GCA CGA GAA TC-3'). Normalization of the amplified samples was obtained by the glyceraldehydes-3-phosphate dehydrogenase (GAPDH) house- keeping gene. For quantitative real-time PCR (QRT-PCR) 100 ng of total RNA were reverse-transcribed using the High-Capacity cDNA Archive Kit (Applied Biosystems) according to the manufacturer's instructions; QRT-PCR was

then performed with an ABI PRISM 7900 sequence detection system (Applied Biosystems). Primers and probes for the different genes' amplification were provided by Applied Biosystems; quantitation was performed by amplifying GAPDH mRNA as endogenous control.

8.4 shRNA human lentivectors

To knockdown ZFP36 expression in human glioma neural stem cells, we used the commercially available pGIPZ-lentiviral shRNAmir vectors containing a hairpin sequence targeting ZFP36 (Open Biosystems, Huntsville, AL). The hairpin sequence was as follows: CGACTTTATTTATTCTAATATTACATCTGTGGCTTCACTAATATTAGAATAAATAA AGTCG.

The shRNA-containing lentiviral vector was cotransfected with lentiviral packaging into HEK-293T cells (Open Biosystems) to produce shRNA-carrying lentivirus particles. Culture supernatants were collected at 48 h after transfection and lentivirus particles were concentrated using PEG (System Biosciences). GNS cells were transduced by the resulting concentrated viral particles (MOI=10) for 1h and after that immediately supplemented with fresh media. After expansion, cells were sorted (MoFlo cell sorter, Beckman Coulter Inc.) based on GFP expression values, obtaining two omogeneous populations expressing either the pGIPZ empty vector or pGIPZ shRNA ZFP36.

8.5 Antibodies and western blots

Cells were lysed with RIPA buffer containing 50 mM TRIS-HCl (pH 7.4), 150 mM NaCl, 1% NP-40, 1 mM sodium deoxycholate, 1 mM sodium orthovanadate and with added 1 mM EDTA and Complete Protease Inhibitor Cocktail (Roche Applied Science); vortexed for 5 sec; and centrifuged at 16,100 g for 30 min at 4°C. Equal amounts of protein were loaded onto 10–12% SDS-polyacrylamide gel, separated by electrophoresis, and transferred to nitrocellulose membranes (GE Healthcare). Expression of actin was analyzed with a mouse anti-human pan-actin MoAb (Sigma-Aldrich) to normalize protein samples. Membranes were probed with ZFP36 polyclonal antibody (Abcam, ab36558), PIM1 polyclonal antibody (Abcam, ab66767), PIM3 polyclonal antibody (Abcam, ab71321), XIAP (Cell Signaling, #2042), Stat5b (G-2) monoclonal antibody (Santa Cruz Biotechnology, sc-1656), RIP1 mouse monoclonal antibody (BD Transduction Laboratories, 610458), Caspase-8 monoclonal antibody (Cell Signaling, 9746), PARP-1 (F-2) (Santa Cruz Biothecnology, sc-8007). Blots were then incubated either with anti-rabbit (Cell Signaling, 7074) or anti-mouse (Santa Cruz Biotechnology, sc-2005) IgG-HRP antibodies and detected using BM Chemiluinescence Blotting Substrate (Roche Applied Science).

8.6 Immunofluorescence

Briefly, cells cultured on coverslips were fixed with 4% paraformaldehyde for 10 min and permeabilized with 0.1% Triton-X 100/PBS for 3 min. Following incubation with ZFP36 primary antibody, cells were washed and incubated with fluorescently labeled secondary antibody Alexa Fluor® 568 (Invitrogen). Finally, nuclei were counterstained by DAPI (Sigma-Aldrich), and slides were analyzed using a Carl Zeiss Axioskop 40 fluorescent microscope (Carl Zeiss).

8.7 Anchorage-independent growth and migration assays

Anchorage-independent growth assays were performed in triplicate in 35mm well plates. 3 x 103 cells per well were seeded in DMEM + 10% FBS containing 0.3% low-melting agarose on the top of the bottom agar containing 0.5% low-melting agarose DMEM + 10% FBS. After 14–21 d colonies were counted. Error bars represent SEM calculated on a set of three to four independent experiments (*$p < 0.05$; **$p < 0.01$). ZFP36 overexpressing cells were first selected by means of puromicyn treatment and then seeded in absence of any selection agent. siRNA transfected ln827 were seeded 72 h after siRNA transfection. For migration assays, cells were cultured at confluence in 24-well plates and then scratched with a thin disposable tip to generate a wound in the cell monolayer. Wound healing

was assessed every 24 h by light microscope.

8.8 Growth curves

Cell growth of G144 ZFP36 KO or G144 treated with cinnamon polyphenols was assessed by a High Definition (HD) imaging system (INCUCYTE™ Live-Cell Imaging System). Cells were monitored in real-time for a total period of 84hrs (KO ZFP36) or 96hrs (C.E.).

8.9 Cell death assays

Apoptotic nuclei were detected by TdT- mediated dUTP terminal nick-end labeling kit (TUNEL) (Roche Applied Science) or by DAPI staining. AnnexinV/PI positivity of indicated cells was assessed by BD PharMingen TM kit (cat. Number 556547). To monitor cell cycle, 1 x 105 cells were suspended in 500 µl hypotonic solution (50 µg/ml PI, 0.1% sodium citrate, 0.1% Triton X-100) and then placed at 4°C in the dark for 10 min before flow cytometry analysis (Coulter Epics XL MCL, Beckman Coulter Inc.).

8.10 Luciferase assays

HEK293 cells were plated at a density of 50,000 cells/well 12 h before transfection in 24-well plates. Transfections were carried using Fugene HD reagent (Roche Applied Science). In a typical assay, each well received 200 ng of pGL3-based reporter construct, 200 ng of CMV-b-galactosidase plasmid (Clontech Laboratories) and 10 ng of pcDNA3.1 FlagZfp36, as indicated in figure legends; the difference in total amount of transfected DNA was scaled up with pcDNA3.1 empty vector. After 24 h, cells were harvested and cell lysates were assayed for luciferase and B-galactosidase activity. Each transfection was done in duplicate in the same experiment, and the plotted luciferase activities represent the average of four different experiments; error bars represent SEM (*$p < 0.05$; **$p < 0.01$).

8.11 Preparation of cinnamon extract

Dried cinnamon (Cinnamomun zeylanicum) was crushed in a mortar. Five g of powder were then suspended in methanol/water (50/50 v/v; 20 ml) and extracted in ultrasound water bath at room temperature for 30 min. The suspension was centrifuged (4,000 rpm), the supernatant was removed, and the solid was extracted again using the same procedure. Liquid phases were then collected and evaporated in vacuo at room temperature to get rid of methanol and finally subjected to freeze drying. The extract yield was

6.1%. All chemicals were reagent grade and used without further purification; they were purchased from Sigma-Aldrich.

9. RESULTS

9.1 ZFP36 expression is low in ln827 and is restored in response to treatment with the de-methylating agent 5-aza cytidine (5 AZA)

The main cell line used in the following experiments is named ln827. This cell line has been established from a high-grade glioma, has tumorigenic features both *in vitro* and *in vivo* and shows an inactivating mutation of p53 plus an inactive splice variant of phosphatase and tensin homolog (PTEN) (Ziegler et al., 2008).

ZFP36 is an early response gene that is transcribed after serum administration (Lai et al., 1998), nevertheless we were not able to observe high levels of ZFP36 mRNA when culturing ln827 in 20% serum (data not shown). Hence we evaluated the ZFP36 gene sequence in UCSC database and noticed the presence of a long stretch of CpG islands covering the entire 5'-proximal promoter region and the single intron of ZFP36 gene (Fig.1rA). CpG islands have been associated with DNA methylation and might influence gene transcription (Jones, 2012). The CpG islands on ZFP36 gene are included in the regions that contain the binding sites for several transcription factors that drive the transcription of ZFP36, therefore we hypothesized that the low expression levels in ln827 might be due to a methylated state of the gene. In order to prove our hypothesis we treated the cell line with the de-methylating agent 5-azacytidine (5-aza) and performed RT-PCR to monitor the levels of ZFP36 mRNAs. The results of the

treatment are shown in Fig.1rB: ZFP36 induction is monitored after treatment with increasing concentrations of 5-aza (2.5, 5 and 10 μM). ZFP36's mRNA levels increase in response to 5-aza with a dose-dependent trend, suggesting that ZFP36 gene might be methylated in the glioblastoma cell line ln827.

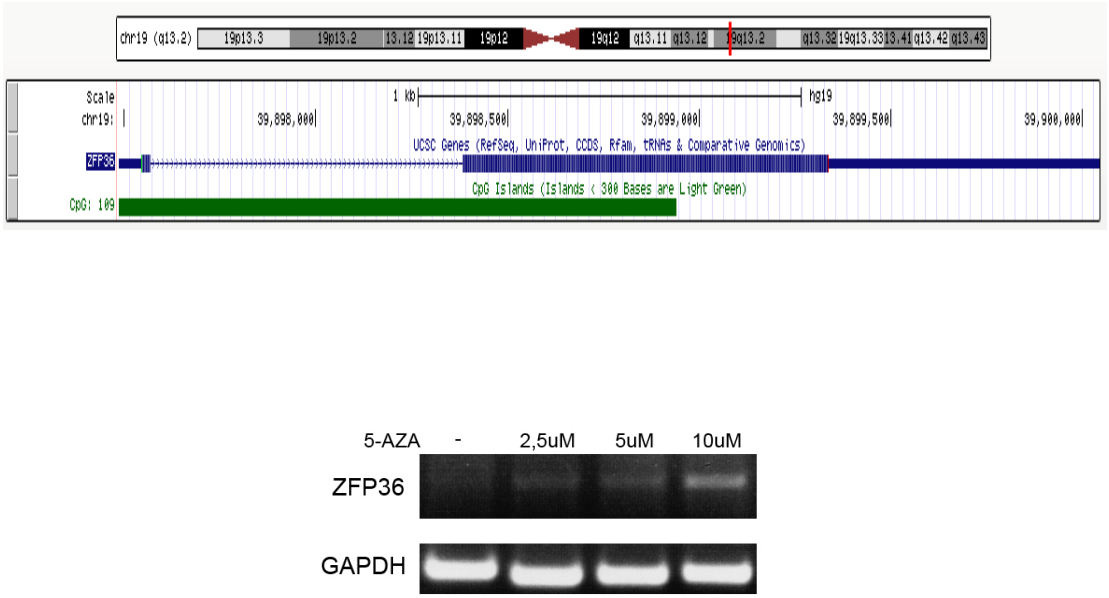

Fig.1r: ZFP36 expression levels are low in ln827 and rise in response to treatment with the de-methylating agent 5-aza cytidine (5-AZA). Figure **A.** represents in green the CpG islands spanning from the proximal promoter region to the second exon of ZFP36 (picture taken from UCSC genome browser). This stretch of CpG islands might be methylated in ln827 leading to ZFP36 down-regulation. Figure **B.** shows the changes in the mRNA levels of ZFP36 and GAPDH in response to the de-methylating agent 5 aza-cytidine (5-aza). The house-keeping gene GAPDH was chosen as endogenous control. The first column shows the effects of vehicle treatment (DMSO), followed by the 2,5-5-10 μM 5aza treatments. Increasing concentration of the de-methylating agent 5-aza induce the expression of ZFP36's mRNA.

9.2 ZFP36 ectopic expression interferes with endogenous levels of XIAP, PIM1 and PIM3 in the GBM cell line ln827

XIAP, PIM1 and PIM3 oncogenes are highly expressed by the glioma cell line ln827 (Fig.2r). By *in silico* analysis of the 3' UTRs we identified AREII sequences that might promote the association of ZFP36 to the mRNAs coding for each of the three oncogenes. Fig.2r A, B, C, D shows the effect of ZFP36 ectopic expression on its putative target genes XIAP, PIM1 and PIM3. In particular, panel A shows a QRT-PCR measuring the ectopic expression of ZFP36 obtained on ln827 cells compared to the empty vector treated population (ln827E.V.). Panel B is a QRT-PCR performed on the same cell populations showing that ln827-ZFP36 cells display lower levels of XIAP, PIM1, PIM3 and Stat5b expression compared to the control population ln827E.V. The analysis of Stat5b expression was included as a control of ZFP36 activity since in a previous work we demonstrated that Stat5b is a target of ZFP36 (Vignudelli et al., 2010). Panel C and D show the same results obtained by different techniques. In particular, panel C shows a semi quantitative RT-PCR and panel D depicts different western blots showing that, following ZFP36 ectopic expression, a decrease in the expression of PIM1, PIM3, XIAP and Stat5b occurs also at the protein level. As a whole, the inverse correlation between the expression of PIM1, PIM3, XIAP and ZFP36, together with the presence of AREII sequences in their 3' untranslated regions (3'UTR) strongly suggests that such genes are indeed ZFP36 direct targets.

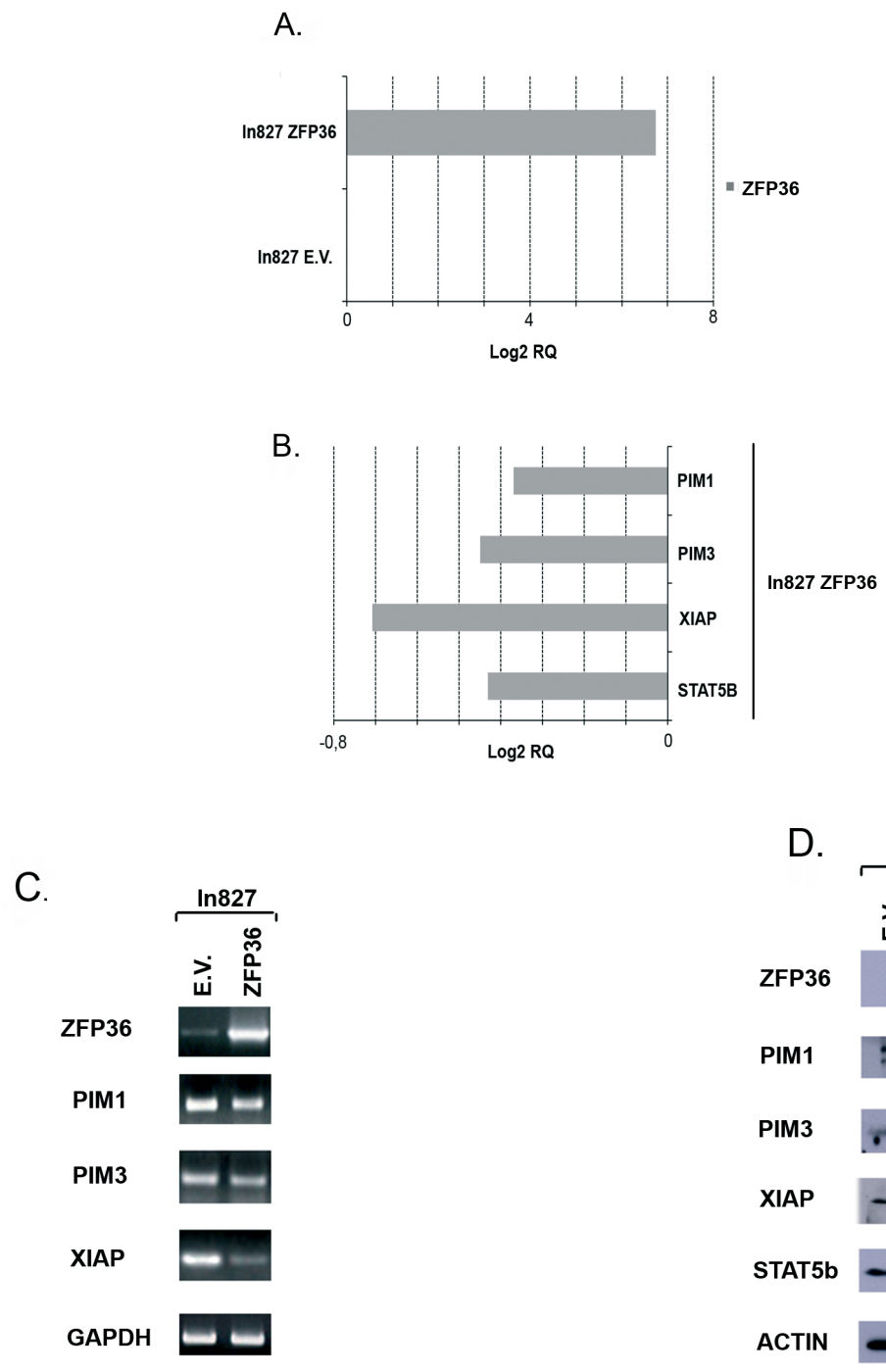

Fig.2r: Overexpression of ZFP36 in the ln827 glioma cell line triggers the degradation of the oncogenic kinases PIM1, PIM3 and of the X-linked inhibitor of apoptosis (XIAP) mRNAs. (**A**) The overexpression levels of ZFP36 in ln827 were assessed by quantitative Real Time PCR (QRT-PCR). (**B**) Following ZFP36 overexpression the mRNAs of PIM1, PIM3 and XIAP are down-modulated. QRT-PCR data are expressed as Log2 of relative quantity compared with the expression levels of the same genes in ln827 cells transfected with empty vector. Stat5b has been used as a positive control for ZFP36 activity. (**C, D**) ln827 cell line expresses high levels of PIM1, PIM3 and XIAP. (**C**) RT-PCR confirms the negative regulation exerted by exogenous ZFP36 on the mRNAs of the targets described in this study. (**D**) In line with the decrease in the mRNA levels, western blots following ZFP36 transduction show a drop in protein levels of PIM1, PIM3, XIAP and Stat5b compared to the E.V. population. All samples were collected 48 hours after transfection with pcDNA3.1 ZFP36 / pcDNA3.1 E.V.

9.3 ZFP36 directly binds PIM1, PIM3 and XIAP 3'-UTRs and thereby affects their stability

Since PIM1, PIM3 and XIAP carry AREII-like nonamers in their 3'UTR regions (Fig.3r), to demonstrate that they are directly targeted by ZFP36, we performed a luciferase reporter assay, generating luciferase reporter constructs (pGL3 based) allowing transcription of a luciferase mRNA carrying the 3'-UTRs of PIM1, PIM3 or XIAP.

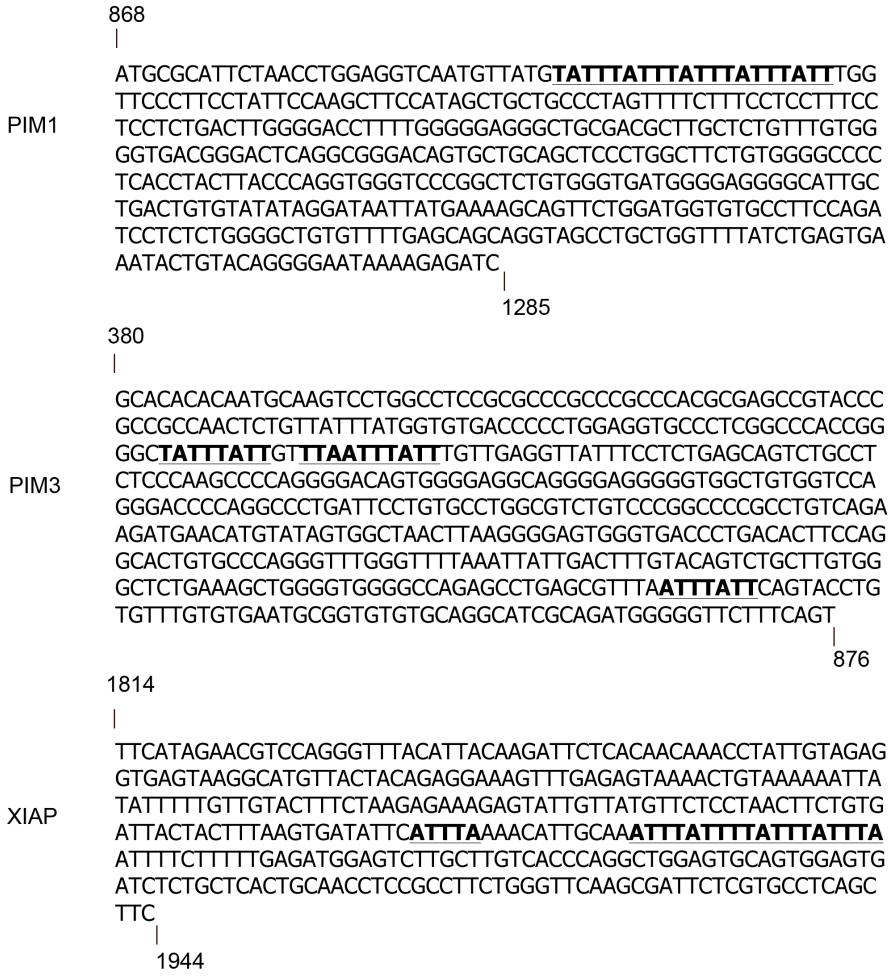

Fig.3r: PIM1, PIM3 and XIAP carry AREII sequences in their 3'UTRs. A portion of 3' UTR containing the AREII sequences was cloned in 3' position of a modified PGL3 luciferase vector. Bp 868 to 1285 of PIM1's 3'UTR (NM_002648) bp 380 to 876 of PIM3's 3'UTR (NM_001001852), bp 1814 to 1944 of XIAP's 3'UTR (NM_001167).

The results are shown in Fig.4r Panel A shows that co-expression of the reporter vector encoding PIM1 3'UTR with a vector expressing ZFP36 significantly decreases the basal reporter activity, demonstrating that by directly binding the described mRNA, ZFP36 impairs protein production by either promoting mRNA degradation or by inhibiting mRNA translation. Panel B and C represent the same kind of experiment performed by co-expressing ZFP36 with the reporter vectors carrying the 3'UTR of PIM3 and XIAP respectively. Again, the assay shows that ZFP36 is capable of directly binding and therefore destabilizing the mRNAs of PIM3 and XIAP.

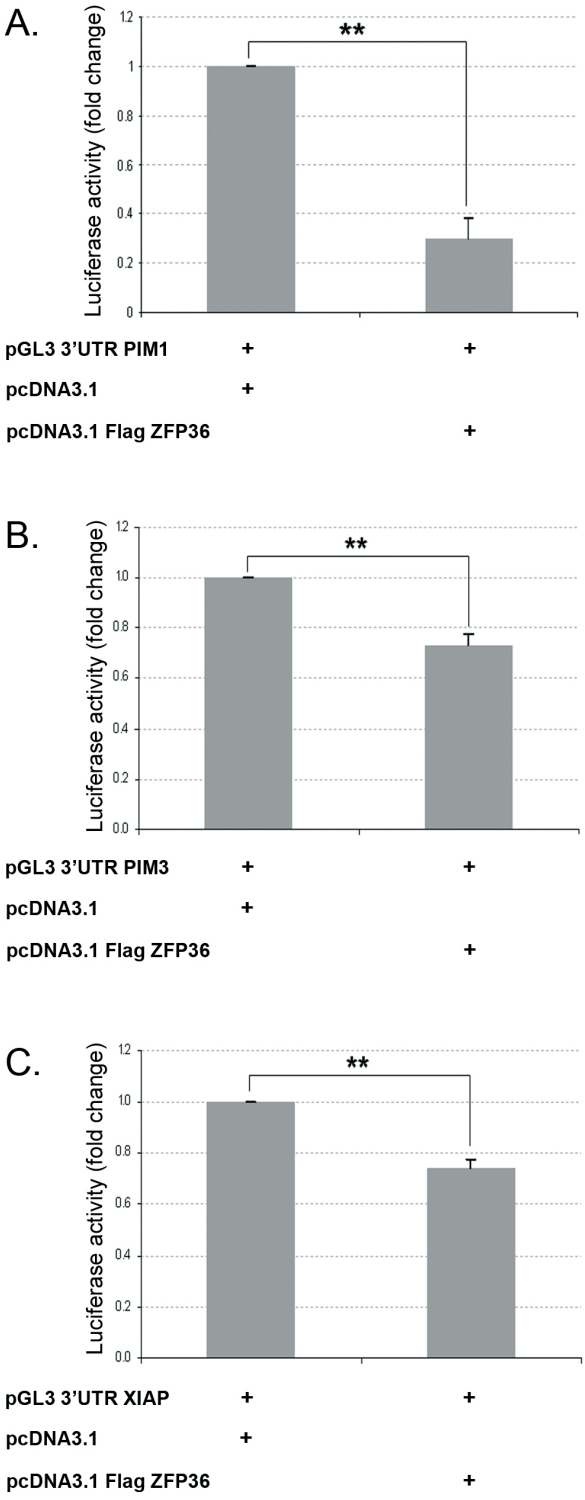

Fig.4r: (A) Luciferase activity assays showing that ZFP36 induces decreased expression of mRNAs carrying the 3'UTR of PIM1, PIM3 or XIAP. (**A**) Luciferase activity was assayed in HEK293 cells transfected with empty pcDNA3.1 vector or with pcDNA3.1 vector expressing FlagZFP36 (10ng) together with pGL3 reporter construct encoding for a luciferase gene fused to the 3'UTR of PIM1. Similar experiments were performed with pcDNA3.1 vector expressing FlagZFP36 together with pGL3 reporter construct encoding for a luciferase gene fused to the 3'UTR of PIM3 (**B**) or XIAP (**C**). Data represent mean and SEM for n=4, **=p<0.01.

9.4 ZFP36 ectopic expression impairs colony formation of ln827 cells

To evaluate if by restoring ZFP36 expression it is possible to impinge on the malignancy of GBM cells, we performed a soft agar assay on ln827 cells over expressing ZFP36 (ln827 ZFP36) and compared them to an empty vector treated sample (ln827E.V.). The results of such experiment are shown in Fig.5r, Panel A shows two pictures suggesting that in the population over-expressing ZFP36, colonies are not only less numerous, but also considerably smaller. Panel B summarizes a series of experiments demonstrating that ZFP36 expression determines a consistent reduction of 30% of colonies compared to the control cell population. Since we hypothesized that the anti-proliferative or death-inducing effect of ZFP36 might reside in its capability of down regulating the expression of target genes such as PIM1, PIM3 and XIAP, we performed soft agar assays on ln827 cells in which these genes were silenced and compared them to ln827 cells treated with a control siRNA (ctr siRNA). The results of such experiment are described in Fig.5r, panels C and D. PIM1, PIM3 and XIAP were silenced singularly or at the same time. Panel C represents a QRT-PCR describing the efficacy of the silencing treatments in the different populations, while panel D shows the numbers of colonies in different sets of experiments. As it was expected, by silencing PIM1, PIM3 and XIAP, a decrease in the number of colonies is observed by soft agar assay and, interestingly, the cumulative silencing determines the strongest impairment of colony formation.

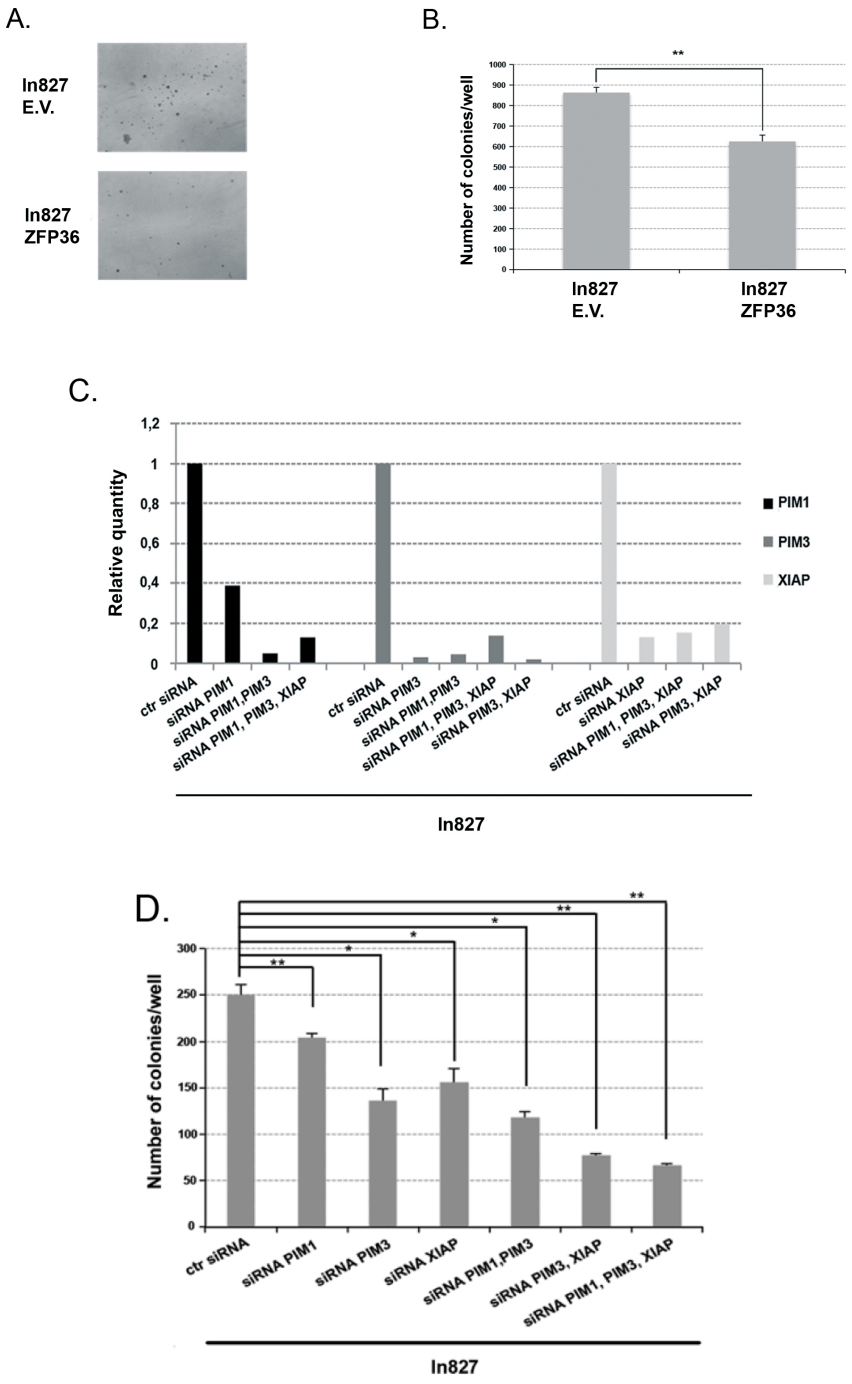

Fig.5r: (**A, B**) **Effect of ZFP36 overexpression on anchorage independent growth in ln827.** After infection and selection for stable transduction, pBABE E.V. and pBABE ZFP36 cells were plated in soft agar. After 21 days colonies were scored. (**A**) 5x magnification phase contrast picture shows the morphology of the scored colonies for each sample. ZFP36 expression induces a strong reduction in size of the grown colonies when compared to the empty vector population. (**B**) ZFP36 expression also impairs the anchorage independent growth of ln827, as demonstrated by the number of scored colonies, which is consistently lower in the ZFP36 population. (**C, D**) Anchorage independent growth of ln827 relies on the expression of PIM1, PIM3 and XIAP. (**C**) QRT-PCR is representative of the efficacy of gene silencing achieved in ln827 through pooled oligo siRNAs transfection. Control siRNA population was set as calibrator in each experiment. (**D**) siRNA transfected cells were plated in soft agar 72 hours after transfection then scored 14 days later. As shown in panel D., single silencing of PIM1, PIM3 or XIAP impairs the colony formation ability of ln827. The concurrent silencing of these genes has a cumulative effect that strongly counteracts the colony formation (The bars in panels B and D represent SEM for three independent experiments, *p<0.05, **p<0.01).

9.5 The decreased colony formation depends on cell death rather than on slower proliferation

To evaluate whether the lower number of colonies observed in the previous assays depends on increased cell death or on a lower proliferation rate, we performed cell cycle analysis and growth curves (data not shown) suggesting that it is not an impairment of proliferation underlying the low number of colonies formed by ln827 cells ectopically expressing ZFP36. Successively, we evaluated by different techniques the viability of the different cell populations. Results of such analysis are summarized in Fig.6r and Fig.7r. In the first experiment (Fig.6r) we performed a count of condensed nuclei, shown in panel A, to generally evaluate the number of cells supposedly undergoing apoptosis. As far as ln827 cells overexpressing ZFP36 are concerned, data are shown in panel B, showing that the percentage of condensed nuclei is consistently 20% higher in ln827 ZFP36 compared to ln827E.V. To complete this set of data we counted nuclei in ln827 cells that previously underwent silencing of PIM1, PIM3 and XIAP. Results are shown in panel C and show that, in accord with soft agar results, the highest death rates are obtained when the target genes are inactivated simultaneously and it has to be underlined that the down-regulation of PIM3 and XIAP seems to be particularly relevant in order to induce cell death.

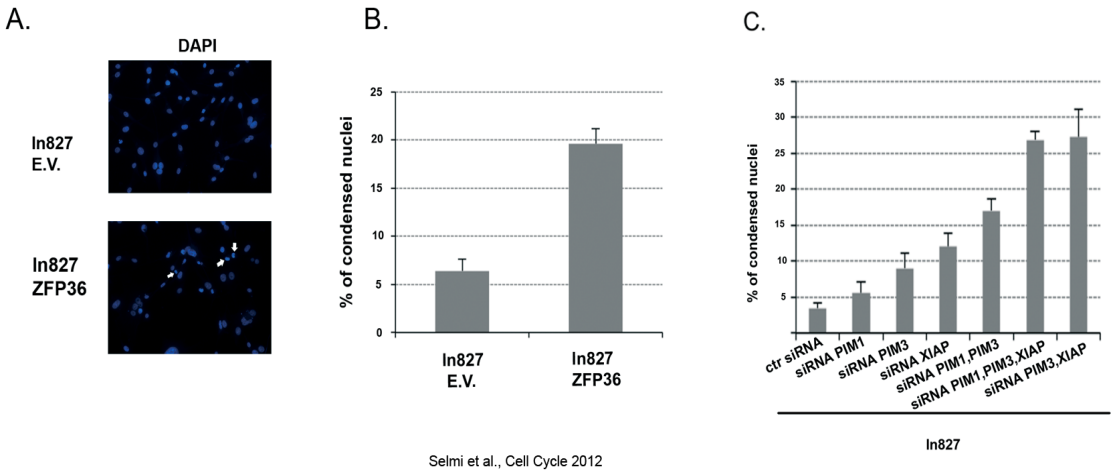

Fig.6r: Condensed nuclei evaluation in ln827E.V. / ZFP36. and in ln827 after PIM1, PIM3 and XIAP depletion by oligo siRNA strategy. (**A**) DAPI staining of pBABE ZFP36 and pBABE E.V. ln827. Cells that undergo ZFP36 overexpression show higher number of both condensed nuclei and micronuclei when compared to the E.V. population. (**B**) ZFP36 population is characterized by a higher frequency of nuclear condensation when compared to the E.V. population. (**C**) Gene silencing by pooled oligo siRNAs of PIM1, PIM3, XIAP reproduces the effect of ZFP36 expression. Again, the multiple silencing of these genes shows to be more effective than the single targeting strategy. The graphs in this figure represent the mean and SEM of n=3 experiments in each of which 10 fields were scored for each cell population. The number of condensed nuclei over the total number of nuclei gives the percentage shown by the graphs.

To assess if the observed death depends on apoptosis, we performed a TUNEL assay on ln827 ZFP36 cells and successively an annexin V/PI assay. Results are shown in Fig.7r. Panel A is an immunofluorescence staining of ZFP36 coupled to the TUNEL assay. Interestingly, a small amount of DNA fragmentation is visible only in cells ectopically expressing ZFP36. To better elucidate the type of cell death, a double staining annexin V-propidium iodide was performed. Results shown in panels B-C were obtained at time points of 24 and 48 hours after infection. Panel B shows that ln827 ZFP36 cells display significantly higher levels of both annexin V and PI positivity compared to the control population ln827E.V. Nevertheless, we were not

able to identify any Annexin V single-positive population at any time point (data not shown), suggesting that the cell death triggered by ZFP36 involves a program that is different from classical apoptosis. We monitored if comparable results could be obtained by silencing PIM1, PIM3 and XIAP in ln827 cells. Data are shown in panel C where the mutual gene silencing of the target genes induces high positivity to annexin V/PI.

Since CASPASE 3 activity was not detected following ZFP36 ectopic expression (data not shown), we hypothesized that XIAP's depletion determined by ZFP36 could lead to ripoptosome aggregation (Tenev et al., 2011) and subsequent death via necroptosis. To verify this hypothesis we performed an immunoblot (panel D) showing that following ZFP36 ectopic expression, ln827 cells display RIPK1 stabilization and low levels of CASP8 activation, represented by the appearance of low molecular weight forms and by a decrease in intensity of the high molecular weight un-cleaved form. Interestingly, we were also able to detect by western blot an increase of a peculiar form of cleaved PARP-1 (Fig.7r E), characterized by the appearance of 116, 55 and 42 KDa bands, compatible with the programmed necrotic cell death (Gobeil et al., 2001).

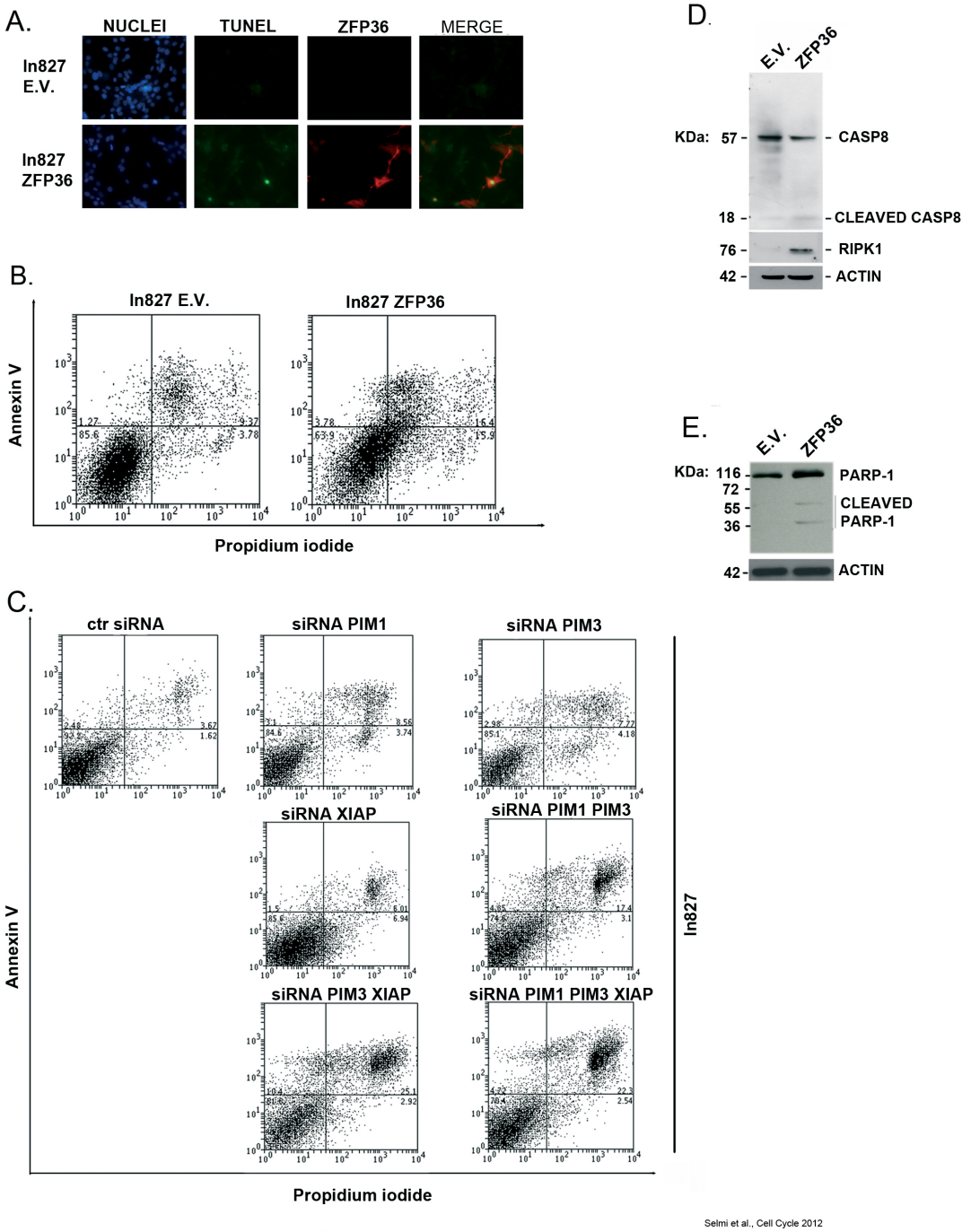

Fig.7r: ZFP36 mediated inhibition of PIM1, PIM3 and XIAP induces necroptotic cell death in glioma cells. (**A**) Transfected ln827 cells were plated on coverslips and 48 hours after transfection they were subjected to TUNEL assay. Positive staining is detected only in the ZFP36 expressing population. (**B**) Cell death was measured at different time points after transduction as the proportion of cells positive for Annexin V and Propidium Iodide. Annexin V values are graphed on the y axis, while PI values are on the x axis. The numbers in the lower right corners represent the percentage of positive cells. Ln827 ZFP36 show increased percentage of both AnnexinV / PI double positive and PI single positive cells. (**C**) Oligo siRNA transfection of the glioma cell line was carried out as described and apoptosis was assessed by Annexin V / PI staining. The single silencing of PIM1, PIM3 and XIAP induces positivity to the apoptotic markers but is less efficient than the simultaneous multiple gene silencing, which strongly increases the percentage of the Annexin V / PI double positive population. (**D**) Western blot analysis shows caspase 8 cleavage and concomitant increase of the RIP1 kinase upon ZFP36 expression. (**E**) Western blot analysis of PARP-1 shows the appearance of 55 KDa and 42 KDa bands in the ln827 ZFP36 population.

9.6 Ectopic expression of ZFP36 reduces the invasion ability of ln827 cells

Since published data suggest that inhibition of Stat5b reduces the invasion potential of human GBM cells (Liang et al., 2009b) and that PIM3 kinase inhibitors down-regulate STAT3(Tyr705) phosphorylation (Chang et al., 2010), thereby impinging on the ability of Stat3 to promote invasion (Lindemann et al., 2011; Senft et al., 2011), we evaluated whether ectopic expression of ZFP36 is capable of reducing invasion by inducing the down regulation of Stat5b and PIM3 simultaneously. To collect evidences to this regard, we performed wound healing assays on ln827 ZFP36 and compared them to ln827E.V. The results are shown in Fig.8r, panel A, where 72 hours after the wound was inflicted, ln827 ZFP36 do not display the same capability to fill the gap as ln827E.V. To demonstrate that the observed impairment in the invasiveness relies on the inactivation of specific targets, we performed other wound healing assays, shown in panel B, on ln827 cells in which PIM3/XIAP or PIM3/PIM1/XIAP were silenced and compared their invasion potential to ln827 treated with a control siRNA. As expected, the populations where PIM1, PIM3 and XIAP were silenced did not show, after 72 hours, the same ability of the control population to repair the wound.

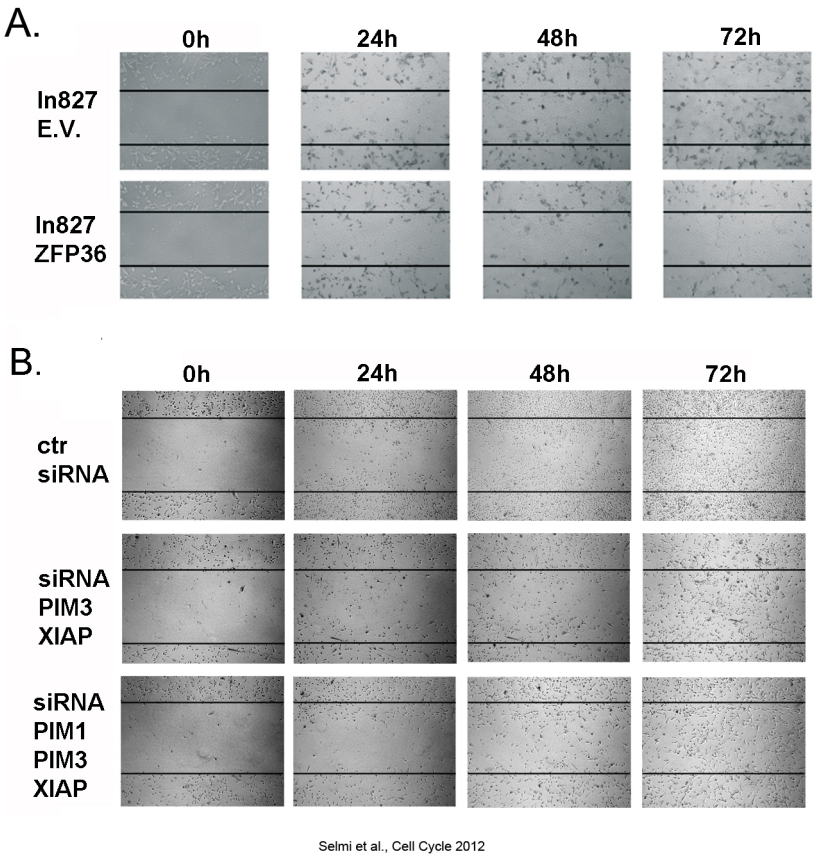

Fig.8r: Migration of glioma cells is inhibited by ZFP36 through down regulation of PIM3 and XIAP. (**A, B**) Wound healing assay was performed as described and cells were checked every 24 hours. Similar results were obtained in 3 independent experiments. ZFP36 expressing cells show a relevant impairment of their migration potential. Silencing of PIM3 and XIAP partially recapitulates this effect.

9.7 Cinnamon polyphenols induce cell death of ln827 cells

To further verify the data collected so far, it was elected to test the biological effect of cinnamon extracts (C.E.), compounds capable of inducing the expression of ZFP36 and other members of the same gene family, (Vignudelli et al., 2010; Cao and Anderson, 2011) on ln827 cells. The data are described in Fig.9r. Panel A represents a QRT-PCR showing

that C.E. induces the expression of ZFP36. In panel B pictures are shown that demonstrate a change in the morphology of ln827 cells treated with C.E. that, following the treatment, detach from the plate. Coupled to the morphological pictures, panel B also carries the DAPI staining of the nuclei clearly showing that condensed apoptotic nuclei are largely represented in the treated population. To confirm the fact that compounds capable of inducing the expression of ZFP36 push ln827 cells toward apoptosis, we performed a cell cycle analysis. The result of this last assay is shown in Fig.9r, panel C, where in the panel representing ln827C.E. a clear sub G1 peak appears, further suggesting that the analyzed population is undergoing cell death.

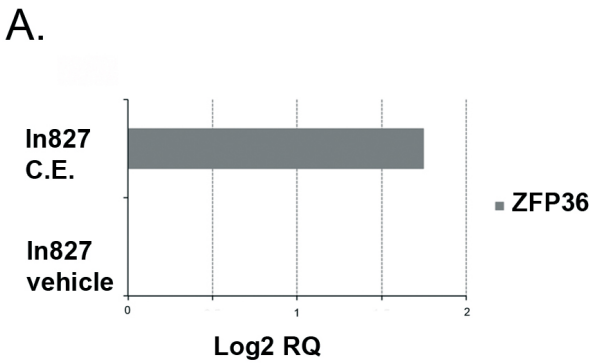

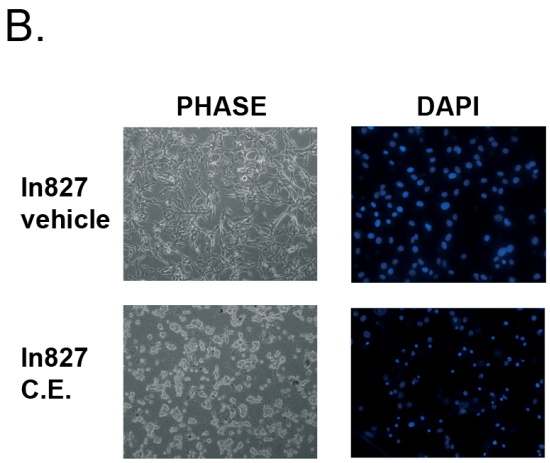

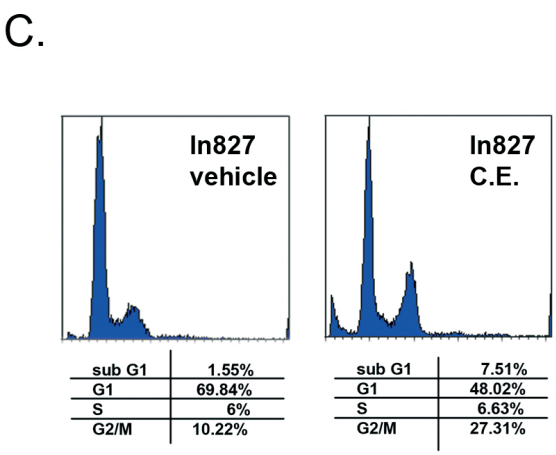

Fig.9r: Cinnamon polyphenols treatment of glioma cells induces ZFP36 expression and reduces cells growth. (**A**) Increase of ZFP36 expression in ln827 was detected by QRT-PCR after 24 hours cinnamon polyphenols treatment at the concentration of 0,25 µg/µl. The vehicle-treated sample was used as calibrator for the basal ZFP36 expression levels. (**B**) Phase contrast images on the left depict the morphology of cinnamon treated glioma at 24 hours treatment. Detachment from the vessel is clearly visible in the lower picture. On the right DAPI staining of similarly treated cells shows an increase of the percentage of condensed nuclei. (**C**) Cell cycle analysis after 24 hours of treatment with polyphenols shows the onset of a sub G1 peak and an increase in the G2/M phase.

9.8 ZFP36 exerts anti-proliferative activity on G144 glioma neural stem cells

Studies performed on embryonic stem cells reveal that ZFP36 is expressed in the undifferentiated state, while it is down-modulated during the differentiation process (Bouhon et al., 2005), but no data regarding the biological significance or the molecular consequences of this variation have been collected so far. Other studies on induced pluripotent stem (iPS) cells revealed that ZFP36 is among the group of genes activated during the acquisition of naïve pluripotency in the absence of additional pluripotency culture requisites (Van Oosten et al., 2012). Hence, we checked the expression of ZFP36 in two different human glioma neural stem cell lines (GNS) that retain the ability to self-renewal, to differentiate and to promote tumor growth after xenotransplantation in mice (Pollard et al., 2009). We did not have access to oligodendroglioma-derived stem cells, which carry the 1p/19q loss and represent the best model to test the effects of ZFP36 re-expression (Huse and Holland, 2010). The two GNS lines used in this study named G144 and G166 both derive from glioblastoma biopsies and none of the two carries the 19q deletion. On the contrary it has been shown that, with respect to G166, G144 have a net gain of two copy of the chromosome 19 (Pollard et al., 2009), possibly leading to an increase of ZFP36 levels. At the biological level, EdU (5-ethynyl-2'-deoxyuridine) incorporation assays reveal that G144 are slow proliferating while G166 are fast cycling, showing half doubling time of G144 (data not shown). No data are available about the PTEN or p53 status in G144 and G166 neither we

investigated this topic. First, we evaluated endogenous ZFP36 in G144 and compared it to G166. The result in Fig.10r, panel A, summarizes data collected by Western Blot, showing that G144 display higher levels of ZFP36 when compared to G166. To elucidate the role of ZFP36 in G144 we knocked down its expression by pGIPZ lentiviral vector carrying a shRNA sequence targeting ZFP36's mRNA (shRNA ZFP36) and, as a control, the same vector carrying a scrambled sequence (pGIPZ). Interestingly, knockdown of ZFP36 (B, C) determines an increase in the proliferation rate of the target population, quantified by growth curve plot (D). We then performed immunoblot analysis of RIPK1 in cells in which ZFP36 expression was depleted and this showed a reduction in the levels of RIPK1, suggesting that ZFP36 could control RIPK1 stability also in the cancer stem cell context (E).

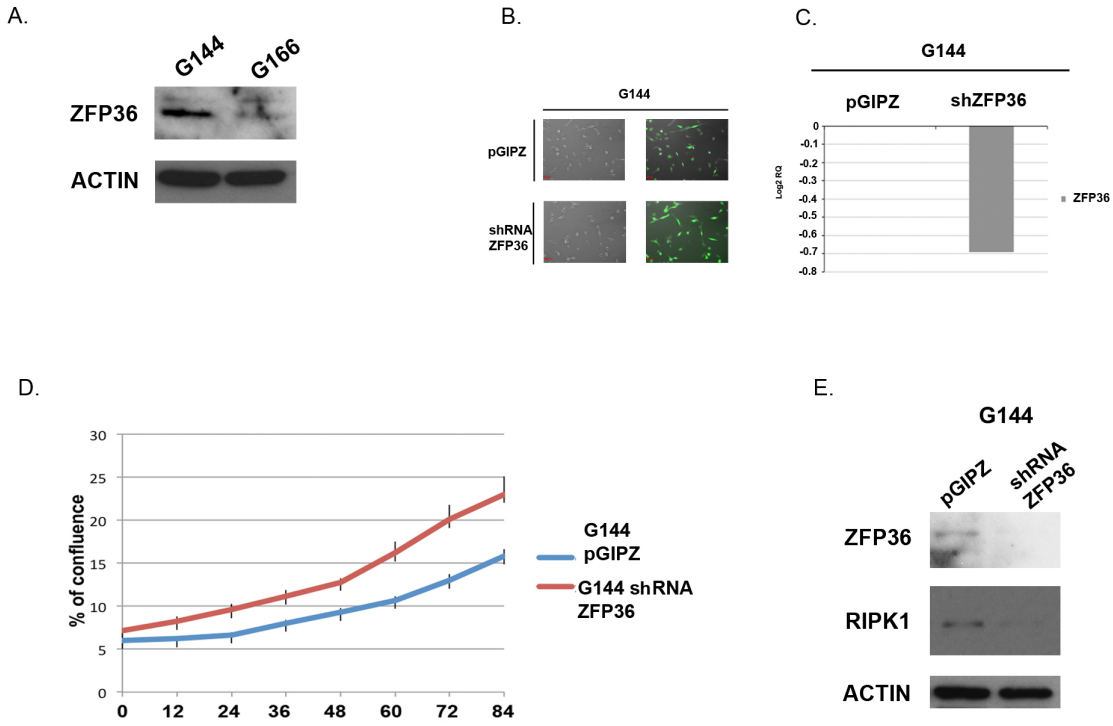

Fig10r: ZFP36 expression in glioma neural stem cells (GNS). (A). G144 express higher levels of endogenous ZFP36 than G166. ACTIN was used as loading control. G144 were infected with a pGIPZ based lentivector carrying a shRNA directed against ZFP36 (G144 shRNA ZFP36) or with a pGIPZ vector carrying a scrambled version of shRNA (G144 pGIPZ), both expressing tGFP under IRES control. Based on GFP expression, cells were sorted to obtain uniform populations (**B**) and quantitative RT-PCR was performed on cDNA collected from G144 pGIPZ and G144 shRNA ZFP36. (**C**). The RT-PCR shows that ZFP36 expression is highly reduced in the G144 shRNA ZFP36 population. The pGIPZ sample was used as a calibrator for the basal ZFP36 expression levels. (**D**) Growth curve performed on the sorted G144 pGIPZ and G144 shRNA ZFP36 suggest that ZFP36 expression influences the proliferation rate of GNS, since the knock down of ZFP36 promotes the proliferative ability of G144. (**E**) Immunoblot showing that knock down of ZFP36 (shRNA ZFP36) associates with a decrease in the stability of RIPK1 if compared to the pGIPZ population.

The efficacy of cinnamon polyphenols in inducing ZFP36 was also tested on G144 glioma neural stem cells. Fig.11r, panel A, is a quantitative RT-PCR performed on G144 treated with two different preparations of cinnamon polyphenols extracts (prep. A and prep. D) at the concentration of 0.01 µg/uL or either at 0.1 µg/uL. Both the preparations promote a dose dependent ZFP36 induction. Fig.11B represents a growth curve that

demonstrates that cinnamon treatment of G144 with the preparation D at the concentration of 0.01 µg/uL exerts an anti-proliferative effect on glioma neural stem cells, possibly due to the increase of the expression levels of ZFP36.

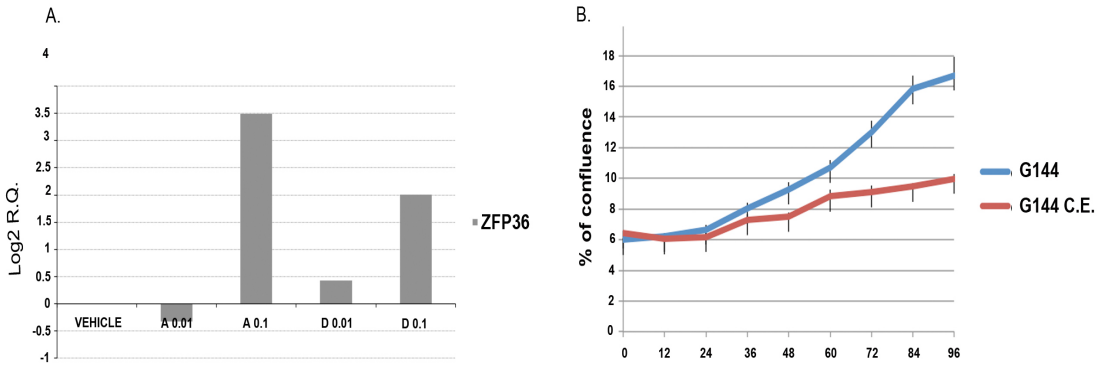

Fig.11r: Cinnamon polyphenols treatment of glioma neural stem cells (GNS) induces ZFP36 and a reduction in proliferation. (**A**) Quantitative RT-PCR shows hat cinnamon polyphenols induce ZFP36 expression in G144. Both preparation A and D displayed high efficacy when used at the concentration of 0.1 µg/uL. Vehicle population was used as internal calibrator of ZFP36 expression levels. (**B**) Growth curve of G144 treated with vehicle in blue or with 0.01 µg/uL preparation D in red (C.E.). Treatment with C.E. reduces the proliferation of G144.

10. DISCUSSION

Although it was originally described as an important regulator of the inflammatory response, a growing body of publications shows that ZFP36 is deficient in cancer cells when compared to normal cell types (Brennan et al., 2009) and that its expression counteracts malignant progression by interfering with different pathways, depending on the disease model (Baou et al., 2009; Sanduja et al., 2009; Cha et al., 2011; Griseri et al., 2011)

The fact that ZFP36 and the other members of this gene family, such as ZFP36L1, are capable of inducing the degradation of quite a large number of mRNAs, among whom are listed those encoding several oncogenes, explains why their targeting seems to be effective in very different and heterogeneous disease models. For this reason, we decided to verify the activity of ZFP36 in GBM cell lines.

GBM is genetically highly heterogeneous and it still has a negative outcome since no effective therapy has been established. Moreover, there is evidence suggesting that ZFP36 is inactivated in gliomas (Suswam et al., 2008) and we collected further evidences (Fig.1r) that in ln827 GBM cell lines ZFP36 is expressed at low levels.

Another aspect strengthening the hypothesis that targeting ZFP36 could impinge on GBM biology, resides on published data suggesting that ZFP36 negatively regulates EGFr pathway (Amit et al., 2007), which is particularly important during the development of the disease, and that among its targets there's also Stat5b (Vignudelli et al., 2010), whose activity

participates in determining the proliferative activity and the invasion capability of GBM cells (Liang et al., 2009b). To verify the effect of ZFP36 expression on GBM cells, we performed ectopic expression experiments and, while doing so, we demonstrated that the kinases PIM1 and PIM3 and X-linked inhibitor of apoptosis protein (XIAP) are new ZFP36 targets.

PIM family's serine/threonine kinases play an important role in cancer biology. Whereas elevated levels of PIM1 and PIM2 are mostly found in hematologic malignancies and prostate cancer, increased PIM3 expression is observed in different solid tumors (Brault et al., 2010). PIM1 and PIM3 are active as oncogenes when their expression increases owing to a loss of regulation, therefore it was reasonable to think that by inducing the expression of a gene capable of determining their down-regulation, ZFP36 by the hypothesis, it would be possible to counteract their oncogenic activity. Among other activities, PIM1 and PIM3 act by repressing apoptosis (Hu et al., 2009; Li et al., 2009; Mukaida et al., 2011; Song and Kraft, 2012) and by stimulating the invasion activity of cancer cells (Santio et al., 2010). These characteristics are reflected in the gene silencing experiments shown here, where down-regulation of PIM1 and PIM3 expression determines cell death and a decrease of invasiveness. In particular, as far as GBM cells are concerned, PIM3 seems to be more relevant than PIM1.

XIAP is an E3 ubiquitine ligase, member of the IAP family, whose other member cIAP2 had already been characterized as a target of ZFP36 (Kim et al., 2010). Although it is clear that IAPs are frequently deregulated in cancer, less clear is how they exert their pro-tumorigenic effect. Recent

data suggest that the E3 ubiquitine ligase activity of IAPs directly influence the assembly of a large death-inducing platform called "ripoptosome" (Tenev et al., 2011) by acting on the stability of the RIP1 kinase in cancer cell lines. Ripoptosome contains the core components RIP1, FADD, and caspase-8, and assembles in response to genotoxic stress-induced depletion of at least two members among XIAP, cIAP1 and cIAP2. Here we show that over-expression of ZFP36 determines the down-regulation of XIAP. We believe that this phenomenon somehow mimics genotoxic stress-induced depletion of IAPs and therefore triggers the assembly of the ripoptosome. This hypothesis is supported by an immunoblot showing an increase in RIP1 following ZFP36 ectopic expression. The increase in the availability of RIP1 might promote the assembly of the ripoptosome. Moreover, only a small proportion of casp8, known as the initiator of the extrinsic apoptotic pathway and also to be a component of ripoptosome-triggered necroptotic cell death, undergoes the pro-activation cleavage, possibly relieving its inhibitory activity on RIP1. In the same cells we also observed a necrotic cleavage of PARP-1, that further suggests that the ZFP36 induced cell death of ln827 GBM cells could depend on a necroptotic cell death program. Altogether, these data suggest that by restoring the expression of ZFP36, ln827 GBM cells die owing to the activation of two distinct death pathways, the one in which PIM1 and PIM3 are involved and the other which is triggered by XIAP's (and cIAP) depletion. Again, this hypothesis is sustained by the silencing experiments, showing that the inactivation of PIM1, PIM3 and XIAP at once is way more effective in inducing cell death than the

single inactivation of the three genes, suggesting that the cumulative effect depends on the activation of different pathways leading to the same biological result, rather than on the interference with a single, common pathway.

Published data show that ZFP36 is expressed by stem cells of different origins and that its expression decreases in response to differentiation, (Bouhon et al., 2005, Van Oosten et al., 2012) but the biological meaning of such regulation still is unanswered. On the basis of our findings we thought that interfering with ZFP36 expression in a cancer stem cell context would have been relevant for proving the conservation of the mechanism of action that we described for ln827. We were not able to test our hypothesis on oligodendroglioma-derived cancer stem cells, which would represent an ideal model since they are characterized by the loss of the long arm of chr19 where Zfp36 gene resides. The stem cell models of our study were instead the glioma neural stem cell lines (GNS) G144 and G166, which have been established from two different glioblastoma biopsies (Pollard et al., 2009). ZFP36 is detectable by immunoblot in the two cell lines and in particular, it seems to be more represented in G144. Following knock down of ZFP36, G144 acquire a faster proliferating rate, indicating that the endogenous ZFP36 has the capability of influencing the growth GNS by a mechanism that we did not investigate, but that might be specific for the stem cell compartment. The death effector RIPK1 is expressed in ln827 as well as in G144. By silencing ZFP36 in G144 we were able to observe a down-modulation of RIPK1, strengthening our hypothesis by which ZFP36

could control the stability of RIP1 by acting on the availability of IAPs proteins. In fact, in the absence of ZFP36, XIAP might be more stable and promote RIP1 degradation via proteasome. This finding reveals that, based on the cell context, ZFP36 could have different effects on the biology of the tumor, in particular one could speculate that endogenous ZFP36 might slow down proliferation in a stem cell context, while ectopic ZFP36 might act by promoting cell death in cell contexts which have lost the stemness properties, such as ln827.

Our last series of experiments shows that when treating the ln827 or the GNS cells with cinnamon polyphenol extracts we were able to up-regulate the expression of ZFP36, that correlated with a reduction of the cell growth of both the cell lines. Therefore, another interesting finding of this work is that ZFP36 is an element that deserves to be considered for the development of future GBM therapies. In fact, since many difficulties encountered while developing new approaches for GBM depend on its heterogeneity, it could be possible to obtain encouraging results by using chemicals capable of inducing the expression of ZFP36. Of particular interest would be restoring ZFP36 expression in oligodendroglioma-derived samples tumors, which are characterized by the loss of Chr 19 (Huse and Holland, 2010) and should present loss of heterozigosity at the Zfp36 allele (Fig.5). Another finding, although merely speculative, that nevertheless deserves to be underlined, regards the ripoptosome. Although so far it was known that this structure appears in response to genotoxic stress, we provide evidence that it might be assembled also following ZFP36

expression in specific cell contexts, and therefore it might represent not only a phenomenon induced by cytotoxic treatments but it could be a physiological event triggered by specific molecular pathways, that surely deserves further investigation.

11. LIST OF ABBREVIATIONS

AGO	argonaute
AMD	ARE-mediated decay
AP-2	activating protein 2
ARE	adenine-uridine rich elements
ARED	Adenine Uridine-rich elements database
Bp	base pair
BRF-1	butyrate response factor-1
BRF-2	butyrate response factor-2
Caf1	chromatin assembly factor 1
CCCH	cystein-cystein-cystein-histidin
Ccr4	carbon catabolite repressor protein 4
CDKN2A	cyclin-dependent kinase inhibitor 2A
C.E.	cinnamon polyphenols extracts
cIAPS	cellular inhibitor of apoptosis proteins
CTD	carboxy-tail domain
CTR	control
Dcp1/Dcp2 cmplex	mRNA-decapping enzyme 1/2 complex
DMSO	dimethyl-sulfoxyde
DP	direct primer
EGF	epidermal growth factor
EGFR	epidermal growth factor receptor
EGR-1	early growth response protein 1

E.V.	empty vector
FADD	FAS-associated death domain protein
FASL	CD95 fas ligand
FLIP	FLICE inhibitory protein
GBM	glioblastoma multiforme
GNSc	glioma neural stem cells
GSCs	glioma stem cells
HCC	hepatocellular carcinoma
HDAC	histone de-acetylase proteins
hEdc3	human enhancer of de-capping 3
HPV18	human papilloma virus 18
HuR	human antigen R (HuR)
IL-8	Interleukin-8
JNK	c-Jun N-terminal kinase
LOH	loss of heterozigosity
MAPK	Mitogen-activated protein kinases
MGMT	O6-methylguanine-DNA-methyltransferase
MYC	homo sapiens v-myc myelocytomatosis viral oncogene homolog (avian)
NEC1	necrostatin1
NES	nuclear export signal
NF-kB	Nuclear factor-kappa beta
NLS	nuclear localization signal
Not	negative on TATA

NTD	amino-tail domain
PARN	poly(A)-specific ribonuclease
PARP1	Poly [ADP-ribose] polymerase 1
PDGFR	platelet derived growth factor
PKB/AKT	protein kinase B
PIM 1,2,3	promielocytic integration site for moloney kinses
PP2A	protein phosphatase 2A
PTEN	phosphatase and tensin homolog
RA	rheumatoid arthritis
RAS	rat sarcoma
RBP	RNA binding protein
RIPK1-3	receptor-interacting serine/threonine-protein kinase 1-3
RP	reverse primer
SMAC	second mitochondria-derived activator of caspases
Smad 3/4	small mother against decapentaplegic proteins 3/4
SNP	single nucleotide polymorfism
SP-1	Specificity Protein 1
STAT3	signal transducer and activator of transcription 3
STAT5b	signal transducer and activator of transcription 5b
SVZ	sub-ventricular zone

TGFb	transforming growth factor beta
Tis11	TPA inducible sequence 11
TNFa	tumor necrosis factor alpha
TRAF2	TNF-receptor-associated factor
TRAIL	TNF-related apoptosis-inducing ligand
TTP	Tristetraprolin
TZFD	tandem zinc finger domains
UTR	un-translated region
VEGF	vascular endothelial growth factor
XIAP	X-linked inhibitor of apoptosis
Xrn1	5'-3' exoribonuclease 1
ZFP36	homo sapiens zinc finger protein 36, C3H type, homolog (mouse)
ZFP36L1	homo sapiens zinc finger protein 36L1, C3H type, homolog (mouse)
ZFP36L2	homo sapiens zinc finger protein 36L2, C3H type, homolog (mouse)

12. REFERENCES

Aho, T.L.T., Sandholm, J., Peltola, K.J., Mankonen, H.P., Lilly, M., and Koskinen, P.J. (2004). Pim-1 kinase promotes inactivation of the pro-apoptotic Bad protein by phosphorylating it on the Ser112 gatekeeper site. FEBS Lett *571*, 43–49.

Al-Souhibani, N., Al-Ahmadi, W., Hesketh, J.E., Blackshear, P.J., and Khabar, K.S.A. (2010). The RNA-binding zinc-finger protein tristetraprolin regulates AU-rich mRNAs involved in breast cancer-related processes. Oncogene *29*, 4205–4215.

Amaravadi, R., and Thompson, C.B. (2005). The survival kinases Akt and Pim as potential pharmacological targets. J Clin Invest *115*, 2618–2624.

Amit, I., Citri, A., Shay, T., Lu, Y., Katz, M., Zhang, F., Tarcic, G., Siwak, D., Lahad, J., Jacob-Hirsch, J., et al. (2007). A module of negative feedback regulators defines growth factor signaling. Nat. Genet. *39*, 503–512.

Anderson, P., and Kedersha, N. (2006). RNA granules. J. Cell Biol. *172*, 803–808.

Anderson, P., and Kedersha, N. (2008). Stress granules: the Tao of RNA triage. Trends Biochem. Sci. *33*, 141–150.

Arribas-Layton, M., Wu, D., Lykke-Andersen, J., and Song, H. (2012). Structural and functional control of the eukaryotic mRNA decapping

machinery. Biochim Biophys Acta.

Bakheet, T., Williams, B.R.G., and Khabar, K.S.A. (2006). ARED 3.0: the large and diverse AU-rich transcriptome. Nucleic Acids Res *34*, D111–D114.

Bao, S., Wu, Q., McLendon, R.E., Hao, Y., Shi, Q., Hjelmeland, A.B., Dewhirst, M.W., Bigner, D.D., and Rich, J.N. (2006). Glioma stem cells promote radioresistance by preferential activation of the DNA damage response. Nature *444*, 756–760.

Baou, M., Jewell, A., Muthurania, A., Wickremasinghe, R.G., Yong, K.L., Carr, R., Marsh, P., and Murphy, J.J. (2009). Involvement of Tis11b, an AU-rich binding protein, in induction of apoptosis by rituximab in B cell chronic lymphocytic leukemia cells. Leukemia *23*, 986–989.

Barrett, L.E., Granot, Z., Coker, C., Iavarone, A., Hambardzumyan, D., Holland, E.C., Nam, H.-S., and Benezra, R. (2012). Self-Renewal Does Not Predict Tumor Growth Potential in Mouse Models of High-Grade Glioma. Cancer Cell *21*, 11–24.

Berghe, T.V., Vanlangenakker, N., Parthoens, E., Deckers, W., Devos, M., Festjens, N., Guerin, C.J., Brunk, U.T., Declercq, W., and Vandenabeele, P. (2009). Necroptosis, necrosis and secondary necrosis converge on similar cellular disintegration features. Cell Death Differ *17*, 922–930.

Bertrand, M.J.M., Milutinovic, S., Dickson, K.M., Ho, W.C., Boudreault, A., Durkin, J., Gillard, J.W., Jaquith, J.B., Morris, S.J., and Barker, P.A. (2008). cIAP1 and cIAP2 facilitate cancer cell survival by functioning as E3 ligases

that promote RIP1 ubiquitination. Mol Cell *30*, 689–700.

Blanco-Aparicio, C., and Carnero, A. (2012). Pim kinases in cancer: Diagnostic, prognostic and treatment opportunities. Biochem Pharmacol.

Bouhon, I.A., Kato, H., Chandran, S., and Allen, N.D. (2005). Neural differentiation of mouse embryonic stem cells in chemically defined medium. Brain Research Bulletin *68*, 62–75.

Brault, L., Gasser, C., Bracher, F., Huber, K., Knapp, S., and Schwaller, J. (2010). PIM serine/threonine kinases in the pathogenesis and therapy of hematologic malignancies and solid cancers. Haematologica *95*, 1004–1015.

Brennan, S.E., Kuwano, Y., Alkharouf, N., Blackshear, P.J., Gorospe, M., and Wilson, G.M. (2009). The mRNA-destabilizing protein tristetraprolin is suppressed in many cancers, altering tumorigenic phenotypes and patient prognosis. Cancer Res *69*, 5168–5176.

Brewer, B.Y., Malicka, J., Blackshear, P.J., and Wilson, G.M. (2004). RNA sequence elements required for high affinity binding by the zinc finger domain of tristetraprolin: conformational changes coupled to the bipartite nature of Au-rich MRNA-destabilizing motifs. J Biol Chem *279*, 27870–27877.

Cao, H., and Anderson, R.A. (2011). Cinnamon polyphenol extract regulates tristetraprolin and related gene expression in mouse adipocytes. J Agric Food Chem *59*, 2739–2744.

Cao, H., Deterding, L.J., Venable, J.D., Kennington, E.A., Yates, J.R., Tomer,

K.B., and Blackshear, P.J. (2006). Identification of the anti-inflammatory protein tristetraprolin as a hyperphosphorylated protein by mass spectrometry and site-directed mutagenesis. Biochem J *394*, 285–297.

Cao, H., Dzineku, F., and Blackshear, P.J. (2003). Expression and purification of recombinant tristetraprolin that can bind to tumor necrosis factor-alpha mRNA and serve as a substrate for mitogen-activated protein kinases. Arch. Biochem. Biophys. *412*, 106–120.

Cao, H., Kelly, M.A., Kari, F., Dawson, H.D., Urban, J.F., Coves, S., Roussel, A.M., and Anderson, R.A. (2007). Green tea increases anti-inflammatory tristetraprolin and decreases pro-inflammatory tumor necrosis factor mRNA levels in rats. J Inflamm (Lond) *4*, 1.

Carballo, E., Lai, W.S., and Blackshear, P.J. (1998). Feedback inhibition of macrophage tumor necrosis factor-alpha production by tristetraprolin. Science *281*, 1001–1005.

Carrick, D.M., and Blackshear, P.J. (2007). Comparative expression of tristetraprolin (TTP) family member transcripts in normal human tissues and cancer cell lines. Arch. Biochem. Biophys. *462*, 278–285.

Carrick, D.M., Chulada, P., Donn, R., Fabris, M., McNicholl, J., Whitworth, W., and Blackshear, P.J. (2006). Genetic variations in ZFP36 and their possible relationship to autoimmune diseases. J. Autoimmun. *26*, 182–196.

Cha, H.J., Lee, H.H., Chae, S.W., Cho, W.J., Kim, Y.M., Choi, H.-J., Choi, D.H., Jung, S.W., Min, Y.J., Lee, B.J., et al. (2011). Tristetraprolin down-

regulates the expression of both VEGF and COX-2 in human colon cancer. Hepatogastroenterology *58*, 790–795.

Chang, M., Kanwar, N., Feng, E., Siu, A., Liu, X., Ma, D., and Jongstra, J. (2010). PIM kinase inhibitors down-regulate STAT3(Tyr705) phosphorylation. Mol Cancer Ther *9*, 2478–2487.

Chen, C.Y., and Shyu, A.B. (1995). AU-rich elements: characterization and importance in mRNA degradation. Trends Biochem. Sci. *20*, 465–470.

Chen, C.Y., Gherzi, R., Ong, S.E., Chan, E.L., Raijmakers, R., Pruijn, G.J., Stoecklin, G., Moroni, C., Mann, M., and Karin, M. (2001). AU binding proteins recruit the exosome to degrade ARE-containing mRNAs. Cell *107*, 451–464.

Cho, Y.S., Challa, S., Moquin, D., Genga, R., Ray, T.D., Guildford, M., and Chan, F.K.-M. (2009). Phosphorylation-driven assembly of the RIP1-RIP3 complex regulates programmed necrosis and virus-induced inflammation. Cell *137*, 1112–1123.

Chrestensen, C.A., Schroeder, M.J., Shabanowitz, J., Hunt, D.F., Pelo, J.W., Worthington, M.T., and Sturgill, T.W. (2004). MAPKAP kinase 2 phosphorylates tristetraprolin on in vivo sites including Ser178, a site required for 14-3-3 binding. J Biol Chem *279*, 10176–10184.

Cougot, N., Babajko, S., and Séraphin, B. (2004). Cytoplasmic foci are sites of mRNA decay in human cells. J. Cell Biol. *165*, 31–40.

Darding, M., and Meier, P. (2012). IAPs: guardians of RIPK1. Cell Death Differ *19*, 58–66.

Darding, M., Feltham, R., Tenev, T., Bianchi, K., Benetatos, C., Silke, J., and Meier, P. (2011). Molecular determinants of Smac mimetic induced degradation of cIAP1 and cIAP2. Cell Death Differ *18*, 1376–1386.

Degterev, A., and Yuan, J. (2008). Expansion and evolution of cell death programmes. Nat Rev Mol Cell Biol *9*, 378–390.

Degterev, A., Hitomi, J., Germscheid, M., Ch'en, I.L., Korkina, O., Teng, X., Abbott, D., Cuny, G.D., Yuan, C., Wagner, G., et al. (2008). Identification of RIP1 kinase as a specific cellular target of necrostatins. Nat. Chem. Biol. *4*, 313–321.

Degterev, A., Huang, Z., Boyce, M., Li, Y., Jagtap, P., Mizushima, N., Cuny, G.D., Mitchison, T.J., Moskowitz, M.A., and Yuan, J. (2005). Chemical inhibitor of nonapoptotic cell death with therapeutic potential for ischemic brain injury. Nat. Chem. Biol. *1*, 112–119.

Doetsch, F., García-Verdugo, J.M., and Alvarez-Buylla, A. (1997). Cellular composition and three-dimensional organization of the subventricular germinal zone in the adult mammalian brain. J Neurosci *17*, 5046–5061.

Du, C., Fang, M., Li, Y., Li, L., and Wang, X. (2000). Smac, a mitochondrial protein that promotes cytochrome c-dependent caspase activation by eliminating IAP inhibition. Cell *102*, 33–42.

DuBois, R.N., McLane, M.W., Ryder, K., Lau, L.F., and Nathans, D. (1990). A growth factor-inducible nuclear protein with a novel cysteine/histidine repetitive sequence. J Biol Chem *265*, 19185–19191.

Fenger-Grøn, M., Fillman, C., Norrild, B., and Lykke-Andersen, J. (2005). Multiple processing body factors and the ARE binding protein TTP activate mRNA decapping. Mol Cell *20*, 905–915.

Feoktistova, M., Geserick, P., Kellert, B., Dimitrova, D.P., Langlais, C., Hupe, M., Cain, K., MacFarlane, M., Häcker, G., and Leverkus, M. (2011). cIAPs Block Ripoptosome Formation, a RIP1/Caspase-8 Containing Intracellular Cell Death Complex Differentially Regulated by cFLIP Isoforms. Mol Cell *43*, 449–463.

Festjens, N., Vanden Berghe, T., and Vandenabeele, P. (2006). Necrosis, a well-orchestrated form of cell demise: signalling cascades, important mediators and concomitant immune response. Biochim Biophys Acta *1757*, 1371–1387.

Franks, T.M., and Lykke-Andersen, J. (2007). TTP and BRF proteins nucleate processing body formation to silence mRNAs with AU-rich elements. Genes Dev *21*, 719–735.

Frederick, L., Wang, X.-Y., Eley, G., and James, C.D. (2000). Diversity and frequency of epidermal growth factor receptor mutations in human glioblastomas. Cancer Res *60*, 1383–1387.

Furnari, F.B., Fenton, T., Bachoo, R.M., Mukasa, A., Stommel, J.M., Stegh,

A., Hahn, W.C., Ligon, K.L., Louis, D.N., Brennan, C., et al. (2007). Malignant astrocytic glioma: genetics, biology, and paths to treatment. Genes Dev *21*, 2683–2710.

Galli, R., Binda, E., Orfanelli, U., Cipelletti, B., Gritti, A., De Vitis, S., Fiocco, R., Foroni, C., Dimeco, F., and Vescovi, A. (2004). Isolation and characterization of tumorigenic, stem-like neural precursors from human glioblastoma. Cancer Res *64*, 7011–7021.

Galluzzi, L., and Kroemer, G. (2008). Necroptosis: a specialized pathway of programmed necrosis. Cell *135*, 1161–1163.

Gebeshuber, C.A., Zatloukal, K., and Martinez, J. (2009). miR-29a suppresses tristetraprolin, which is a regulator of epithelial polarity and metastasis. EMBO Rep *10*, 400–405.

Gobeil, S., Boucher, C.C., Nadeau, D., and Poirier, G.G. (2001). Characterization of the necrotic cleavage of poly(ADP-ribose) polymerase (PARP-1): implication of lysosomal proteases. Cell Death Differ *8*, 588–594.

Gomperts, M., Corps, A.N., Pascall, J.C., and Brown, K.D. (1992). Mitogen-induced expression of the primary response gene cMG1 in a rat intestinal epithelial cell-line (RIE-1). FEBS Lett *306*, 1–4.

Griseri, P., Bourcier, C., Hieblot, C., Essafi-Benkhadir, K., Chamorey, E., Touriol, C., and Pagès, G. (2011). A synonymous polymorphism of the Tristetraprolin (TTP) gene, an AU-rich mRNA-binding protein, affects translation efficiency and response to Herceptin treatment in breast cancer

patients. Hum Mol Genet *20*, 4556–4568.

Gyrd-Hansen, M., and Meier, P. (2010). IAPs: from caspase inhibitors to modulators of NF-kappaB, inflammation and cancer. Nat Rev Cancer *10*, 561–574.

Hanahan, D., and Weinberg, R.A. (2011). Hallmarks of cancer: the next generation. Cell *144*, 646–674.

Hau, H.H., Walsh, R.J., Ogilvie, R.L., Williams, D.A., Reilly, C.S., and Bohjanen, P.R. (2007). Tristetraprolin recruits functional mRNA decay complexes to ARE sequences. J Cell Biochem *100*, 1477–1492.

He, S., Nakada, D., and Morrison, S.J. (2009a). Mechanisms of stem cell self-renewal. Annu. Rev. Cell Dev. Biol. *25*, 377–406.

He, S., Wang, L., Miao, L., Wang, T., Du, F., Zhao, L., and Wang, X. (2009b). Receptor interacting protein kinase-3 determines cellular necrotic response to TNF-alpha. Cell *137*, 1100–1111.

Hemmati, H.D., Nakano, I., Lazareff, J.A., Masterman-Smith, M., Geschwind, D.H., Bronner-Fraser, M., and Kornblum, H.I. (2003). Cancerous stem cells can arise from pediatric brain tumors. Proc Natl Acad Sci USA *100*, 15178–15183.

Hitti, E., Iakovleva, T., Brook, M., Deppenmeier, S., Gruber, A.D., Radzioch, D., Clark, A.R., Blackshear, P.J., Kotlyarov, A., and Gaestel, M. (2006). Mitogen-activated protein kinase-activated protein kinase 2 regulates tumor

necrosis factor mRNA stability and translation mainly by altering tristetraprolin expression, stability, and binding to adenine/uridine-rich element. Mol Cell Biol *26*, 2399–2407.

Holcik, M., and Korneluk, R.G. (2001). XIAP, the guardian angel. Nat Rev Mol Cell Biol *2*, 550–556.

Holcik, M., Yeh, C., Korneluk, R.G., and Chow, T. (2000). Translational upregulation of X-linked inhibitor of apoptosis (XIAP) increases resistance to radiation induced cell death. Oncogene *19*, 4174–4177.

Holler, N., Zaru, R., Micheau, O., Thome, M., Attinger, A., Valitutti, S., Bodmer, J.L., Schneider, P., Seed, B., and Tschopp, J. (2000). Fas triggers an alternative, caspase-8-independent cell death pathway using the kinase RIP as effector molecule. Nat Immunol *1*, 489–495.

Hsu, H., Xiong, J., and Goeddel, D.V. (1995). The TNF receptor 1-associated protein TRADD signals cell death and NF-kappa B activation. Cell *81*, 495–504.

Hu, X.F., Li, J., Vandervalk, S., Wang, Z., Magnuson, N.S., and Xing, P.X. (2009). PIM-1-specific mAb suppresses human and mouse tumor growth by decreasing PIM-1 levels, reducing Akt phosphorylation, and activating apoptosis. J Clin Invest *119*, 362–375.

Huse, J.T., and Holland, E.C. (2010). Targeting brain cancer: advances in the molecular pathology of malignant glioma and medulloblastoma. Nat Rev Cancer *10*, 319–331.

Ishmael, F.T., Fang, X., Galdiero, M.R., Atasoy, U., Rigby, W.F.C., Gorospe, M., Cheadle, C., and Stellato, C. (2008). Role of the RNA-binding protein tristetraprolin in glucocorticoid-mediated gene regulation. J Immunol *180*, 8342–8353.

Jing, Q., Huang, S., Guth, S., Zarubin, T., Motoyama, A., Chen, J., Di Padova, F., Lin, S.-C., Gram, H., and Han, J. (2005). Involvement of microRNA in AU-rich element-mediated mRNA instability. Cell *120*, 623–634.

Johnson, B.A., Stehn, J.R., Yaffe, M.B., and Blackwell, T.K. (2002). Cytoplasmic localization of tristetraprolin involves 14-3-3-dependent and -independent mechanisms. J Biol Chem *277*, 18029–18036.

Jones, P.A. (2012). Functions of DNA methylation: islands, start sites, gene bodies and beyond. Nat Rev Genet *13*, 484–492.

Kedersha, N., Stoecklin, G., Ayodele, M., Yacono, P., Lykke-Andersen, J., Fritzler, M.J., Scheuner, D., Kaufman, R.J., Golan, D.E., and Anderson, P. (2005). Stress granules and processing bodies are dynamically linked sites of mRNP remodeling. J. Cell Biol. *169*, 871–884.

Khabar, K.S.A. (2005). The AU-rich transcriptome: more than interferons and cytokines, and its role in disease. J. Interferon Cytokine Res. *25*, 1–10.

Khabar, K.S.A. (2010). Post-transcriptional control during chronic inflammation and cancer: a focus on AU-rich elements. Cell. Mol. Life Sci. *67*, 2937–2955.

Kim, C.W., Kim, H.K., Vo, M.-T., Lee, H.H., Kim, H.J., Min, Y.J., Cho, W.J., and Park, J.W. (2010). Tristetraprolin controls the stability of cIAP2 mRNA through binding to the 3'UTR of cIAP2 mRNA. Biochem Biophys Res Commun.

Krakstad, C., and Chekenya, M. (2010). Survival signalling and apoptosis resistance in glioblastomas: opportunities for targeted therapeutics. Mol Cancer *9*, 135.

Kreuzaler, P., and Watson, C.J. (2012). Killing a cancer: what are the alternatives? Nat Rev Cancer *12*, 411–424.

Krueger, A., Schmitz, I., Baumann, S., Krammer, P.H., and Kirchhoff, S. (2001). Cellular FLICE-inhibitory protein splice variants inhibit different steps of caspase-8 activation at the CD95 death-inducing signaling complex. J Biol Chem *276*, 20633–20640.

Lai, W.S., Carballo, E., Strum, J.R., Kennington, E.A., Phillips, R.S., and Blackshear, P.J. (1999). Evidence that tristetraprolin binds to AU-rich elements and promotes the deadenylation and destabilization of tumor necrosis factor alpha mRNA. Mol Cell Biol *19*, 4311–4323.

Lai, W.S., Carballo, E., Thorn, J.M., Kennington, E.A., and Blackshear, P.J. (2000). Interactions of CCCH zinc finger proteins with mRNA. Binding of tristetraprolin-related zinc finger proteins to Au-rich elements and destabilization of mRNA. J Biol Chem *275*, 17827–17837.

Lai, W.S., Kennington, E.A., and Blackshear, P.J. (2002). Interactions of

CCCH zinc finger proteins with mRNA: non-binding tristetraprolin mutants exert an inhibitory effect on degradation of AU-rich element-containing mRNAs. J Biol Chem *277*, 9606–9613.

Lai, W.S., Kennington, E.A., and Blackshear, P.J. (2003). Tristetraprolin and its family members can promote the cell-free deadenylation of AU-rich element-containing mRNAs by poly(A) ribonuclease. Mol Cell Biol *23*, 3798–3812.

Lai, W.S., Stumpo, D.J., and Blackshear, P.J. (1990). Rapid insulin-stimulated accumulation of an mRNA encoding a proline-rich protein. J Biol Chem *265*, 16556–16563.

Lai, W.S., Thompson, M.J., and Blackshear, P.J. (1998). Characteristics of the intron involvement in the mitogen-induced expression of Zfp-36. J Biol Chem *273*, 506–517.

Lai, W.S., Thompson, M.J., Taylor, G.A., Liu, Y., and Blackshear, P.J. (1995). Promoter analysis of Zfp-36, the mitogen-inducible gene encoding the zinc finger protein tristetraprolin. J Biol Chem *270*, 25266–25272.

Laster, S.M., Wood, J.G., and Gooding, L.R. (1988). Tumor necrosis factor can induce both apoptic and necrotic forms of cell lysis. J Immunol *141*, 2629–2634.

Lemaire, C., Andréau, K., Souvannavong, V., and Adam, A. (1998). Inhibition of caspase activity induces a switch from apoptosis to necrosis. FEBS Lett *425*, 266–270.

Li, J., Hu, X.F., Loveland, B.E., and Xing, P.X. (2009). Pim-1 expression and monoclonal antibody targeting in human leukemia cell lines. Exp Hematol *37*, 1284–1294.

Liang, J., Lei, T., Song, Y., Yanes, N., Qi, Y., and Fu, M. (2009a). RNA-destabilizing factor tristetraprolin negatively regulates NF-kappaB signaling. J Biol Chem *284*, 29383–29390.

Liang, Q.-C., Xiong, H., Zhao, Z.-W., Jia, D., Li, W.-X., Qin, H.-Z., Deng, J.-P., Gao, L., Zhang, H., and Gao, G.-D. (2009b). Inhibition of transcription factor STAT5b suppresses proliferation, induces G1 cell cycle arrest and reduces tumor cell invasion in human glioblastoma multiforme cells. Cancer Lett *273*, 164–171.

Lilly, M., Sandholm, J., Cooper, J.J., Koskinen, P.J., and Kraft, A. (1999). The PIM-1 serine kinase prolongs survival and inhibits apoptosis-related mitochondrial dysfunction in part through a bcl-2-dependent pathway. Oncogene *18*, 4022–4031.

Lindemann, C., Hackmann, O., Delic, S., Schmidt, N., Reifenberger, G., and Riemenschneider, M.J. (2011). SOCS3 promoter methylation is mutually exclusive to EGFR amplification in gliomas and promotes glioma cell invasion through STAT3 and FAK activation. Acta Neuropathol. *122*, 241–251.

Louis, D.N. (2006). Molecular pathology of malignant gliomas. Annu Rev Pathol *1*, 97–117.

Lu, J.V., Weist, B.M., van Raam, B.J., Marro, B.S., Nguyen, L.V., Srinivas, P., Bell, B.D., Luhrs, K.A., Lane, T.E., Salvesen, G.S., et al. (2011). Complementary roles of Fas-associated death domain (FADD) and receptor interacting protein kinase-3 (RIPK3) in T-cell homeostasis and antiviral immunity. Proc Natl Acad Sci USA *108*, 15312–15317.

Lykke-Andersen, J., and Wagner, E. (2005). Recruitment and activation of mRNA decay enzymes by two ARE-mediated decay activation domains in the proteins TTP and BRF-1. Genes Dev *19*, 351–361.

Maher, E.A., Furnari, F.B., Bachoo, R.M., Rowitch, D.H., Louis, D.N., Cavenee, W.K., and DePinho, R.A. (2001). Malignant glioma: genetics and biology of a grave matter. Genes Dev *15*, 1311–1333.

Mahtani, K.R., Brook, M., Dean, J.L., Sully, G., Saklatvala, J., and Clark, A.R. (2001). Mitogen-activated protein kinase p38 controls the expression and posttranslational modification of tristetraprolin, a regulator of tumor necrosis factor alpha mRNA stability. Mol Cell Biol *21*, 6461–6469.

Mannino, M., and Chalmers, A.J. (2011). Radioresistance of glioma stem cells: Intrinsic characteristic or property of the 'microenvironment-stem cell unit'? Mol Oncol *5 (4)*, 374-386.

Marchese, F.P., Aubareda, A., Tudor, C., Saklatvala, J., Clark, A.R., and Dean, J.L.E. (2010). MAPKAP kinase 2 blocks tristetraprolin-directed mRNA decay by inhibiting CAF1 deadenylase recruitment. J Biol Chem *285*, 27590–27600.

Marderosian, M., Sharma, A., Funk, A.P., Vartanian, R., Masri, J., Jo, O.D., and Gera, J.F. (2006). Tristetraprolin regulates Cyclin D1 and c-Myc mRNA stability in response to rapamycin in an Akt-dependent manner via p38 MAPK signaling. Oncogene *25*, 6277–6290.

Micheau, O., and Tschopp, J. (2003). Induction of TNF receptor I-mediated apoptosis via two sequential signaling complexes. Cell *114*, 181–190.

Mikkers, H., Nawijn, M., Allen, J., Brouwers, C., Verhoeven, E., Jonkers, J., and Berns, A. (2004). Mice deficient for all PIM kinases display reduced body size and impaired responses to hematopoietic growth factors. Mol Cell Biol *24*, 6104–6115.

Mischel, P.S., Shai, R., Shi, T., Horvath, S., Lu, K.V., Choe, G., Seligson, D., Kremen, T.J., Palotie, A., Liau, L.M., et al. (2003). Identification of molecular subtypes of glioblastoma by gene expression profiling. Oncogene *22*, 2361–2373.

Mukaida, N., Wang, Y.-Y., and Li, Y.-Y. (2011). Roles of Pim-3, a novel survival kinase, in tumorigenesis. Cancer Sci. *102*, 1437–1442.

Murata, T., Morita, N., Hikita, K., Kiuchi, K., Kiuchi, K., and Kaneda, N. (2005). Recruitment of mRNA-destabilizing protein TIS11 to stress granules is mediated by its zinc finger domain. Exp Cell Res *303*, 287–299.

Galban., and Duckett, C.S. (2009). XIAP as a ubiquitin ligase in cellular signaling. Cell Death Differ *17*, 54–60.

Nawijn, M.C., Alendar, A., and Berns, A. (2011). For better or for worse: the role of Pim oncogenes in tumorigenesis. Nat Rev Cancer *11*, 23–34.

Oberst, A., Dillon, C.P., Weinlich, R., McCormick, L.L., Fitzgerald, P., Pop, C., Hakem, R., Salvesen, G.S., and Green, D.R. (2011). Catalytic activity of the caspase-8-FLIP(L) complex inhibits RIPK3-dependent necrosis. Nature *471*, 363–367.

Ogawa, K., Chen, F., Kim, Y.-J., and Chen, Y. (2003). Transcriptional regulation of tristetraprolin by transforming growth factor-beta in human T cells. J Biol Chem *278*, 30373–30381.

Phillips, H.S., Kharbanda, S., Chen, R., Forrest, W.F., Soriano, R.H., Wu, T.D., Misra, A., Nigro, J.M., Colman, H., Soroceanu, L., et al. (2006). Molecular subclasses of high-grade glioma predict prognosis, delineate a pattern of disease progression, and resemble stages in neurogenesis. Cancer Cell *9*, 157–173.

Phillips, R.S. (2002). Members of the Tristetraprolin Family of Tandem CCCH Zinc Finger Proteins Exhibit CRM1-dependent Nucleocytoplasmic Shuttling. Journal of Biological Chemistry *277*, 11606–11613.

Piccirillo, S.G.M., Reynolds, B.A., Zanetti, N., Lamorte, G., Binda, E., Broggi, G., Brem, H., Olivi, A., Dimeco, F., and Vescovi, A.L. (2006). Bone morphogenetic proteins inhibit the tumorigenic potential of human brain tumour-initiating cells. Nature *444*, 761–765.

Pikarsky, E., Porat, R.M., Stein, I., Abramovitch, R., Amit, S., Kasem, S.,

Gutkovich-Pyest, E., Urieli-Shoval, S., Galun, E., and Ben-Neriah, Y. (2004). NF-kappaB functions as a tumour promoter in inflammation-associated cancer. Nature *431*, 461–466.

Pillai, R.S. (2005). MicroRNA function: multiple mechanisms for a tiny RNA? Rna *11*, 1753–1761.

Pollard, S.M., Yoshikawa, K., Clarke, I.D., Danovi, D., Stricker, S., Russell, R., Bayani, J., Head, R., Lee, M., Bernstein, M., et al. (2009). Glioma stem cell lines expanded in adherent culture have tumor-specific phenotypes and are suitable for chemical and genetic screens. Cell Stem Cell *4*, 568–580.

Prchal, J.F., Adamson, J.W., Murphy, S., Steinmann, L., and Fialkow, P.J. (1978). Polycythemia vera. The in vitro response of normal and abnormal stem cell lines to erythropoietin. J Clin Invest *61*, 1044–1047.

Raychaudhuri, B., and Vogelbaum, M.A. (2011). IL-8 is a mediator of NF-κB induced invasion by gliomas. J Neurooncol *101*, 227–235.

Reifenberger, J., Reifenberger, G., Liu, L., James, C.D., Wechsler, W., and Collins, V.P. (1994). Molecular genetic analysis of oligodendroglial tumors shows preferential allelic deletions on 19q and 1p. Am J Pathol *145*, 1175–1190.

Reya, T., Morrison, S.J., Clarke, M.F., and Weissman, I.L. (2001). Stem cells, cancer, and cancer stem cells. Nature *414*, 105–111.

Riley, A., Jordan, L.E., and Holcik, M. (2010). Distinct 5' UTRs regulate XIAP

expression under normal growth conditions and during cellular stress. Nucleic Acids Res *38*, 4665–4674.

Rounbehler, R.J., Fallahi, M., Yang, C., Steeves, M.A., Li, W., Doherty, J.R., Schaub, F.X., Sanduja, S., Dixon, D.A., Blackshear, P.J., et al. (2012). Tristetraprolin impairs myc-induced lymphoma and abolishes the malignant state. Cell *150*, 563–574.

Sandler, H., Kreth, J., Timmers, H.T.M., and Stoecklin, G. (2011). Not1 mediates recruitment of the deadenylase Caf1 to mRNAs targeted for degradation by tristetraprolin. Nucleic Acids Res *39*, 4373–4386.

Sanduja, S., Blanco, F.F., Young, L.E., Kaza, V., and Dixon, D.A. (2012). The role of tristetraprolin in cancer and inflammation. Front. Biosci. *17*, 174–188.

Sanduja, S., Kaza, V., and Dixon, D.A. (2009). The mRNA decay factor tristetraprolin (TTP) induces senescence in human papillomavirus-transformed cervical cancer cells by targeting E6-AP ubiquitin ligase. Aging (Albany NY) *1*, 803–817.

Santio, N.M., Vahakoski, R.L., Rainio, E.-M., Sandholm, J.A., Virtanen, S.S., Prudhomme, M., Anizon, F., Moreau, P., and Koskinen, P.J. (2010). Pim-selective inhibitor DHPCC-9 reveals Pim kinases as potent stimulators of cancer cell migration and invasion. Mol Cancer *9*, 279.

Scheffler, B., Walton, N.M., Lin, D.D., Goetz, A.K., Enikolopov, G., Roper, S.N., and Steindler, D.A. (2005). Phenotypic and functional characterization

of adult brain neuropoiesis. Proc Natl Acad Sci USA *102*, 9353–9358.

Schichl, Y.M., Resch, U., Hofer-Warbinek, R., and de Martin, R. (2009). Tristetraprolin impairs NF-kappaB/p65 nuclear translocation. J Biol Chem *284*, 29571–29581.

Schichl, Y.M., Resch, U., Lemberger, C.E., Stichlberger, D., and de Martin, R. (2011). Novel phosphorylation-dependent Ubiquitination of Tristetraprolin by MEK kinase 1 (MEKK1) and TNF-receptor associated factor 2 (TRAF2). J Biol Chem. *286,* 38466-38477.

Selmi, T., Martello, A., Vignudelli, T., Ferrari, E., Grande, A., Gemelli, C., Salomoni, P., Ferrari, S., and Zanocco-Marani, T. (2012). ZFP36 expression impairs glioblastoma cell lines viability and invasiveness by targeting multiple signal transduction pathways. Cell Cycle *11(10)*, 1977-1987.

Senft, C., Polacin, M., Priester, M., Seifert, V., Kögel, D., and Weissenberger, J. (2010). The nontoxic natural compound Curcumin exerts anti-proliferative, anti-migratory, and anti-invasive properties against malignant gliomas. BMC Cancer *10*, 491.

Senft, C., Priester, M., Polacin, M., Schröder, K., Seifert, V., Kögel, D., and Weissenberger, J. (2011). Inhibition of the JAK-2/STAT3 signaling pathway impedes the migratory and invasive potential of human glioblastoma cells. J Neurooncol *101*, 393–403.

Siegelin, M.D., Gaiser, T., and Siegelin, Y. (2009). The XIAP inhibitor Embelin enhances TRAIL-mediated apoptosis in malignant glioma cells by

down-regulation of the short isoform of FLIP. Neurochem. Int. *55*, 423–430.

Singh, S.K., Clarke, I.D., Hide, T., and Dirks, P.B. (2004). Cancer stem cells in nervous system tumors. Oncogene *23*, 7267–7273.

Singh, S.K., Clarke, I.D., Terasaki, M., Bonn, V.E., Hawkins, C., Squire, J., and Dirks, P.B. (2003). Identification of a cancer stem cell in human brain tumors. Cancer Res *63*, 5821–5828.

Smith, J.S., Alderete, B., Minn, Y., Borell, T.J., Perry, A., Mohapatra, G., Hosek, S.M., Kimmel, D., O'Fallon, J., Yates, A., et al. (1999). Localization of common deletion regions on 1p and 19q in human gliomas and their association with histological subtype. Oncogene *18*, 4144–4152.

Sohn, B.H., Park, I.Y., Lee, J.J., Yang, S.-J., Jang, Y.J., Park, K.C., Kim, D.J., Lee, D.C., Sohn, H.A., Kim, T.W., et al. (2010). Functional switching of TGF-beta1 signaling in liver cancer via epigenetic modulation of a single CpG site in TTP promoter. Gastroenterology *138*, 1898–1908.

Song, J.H., and Kraft, A.S. (2012). Pim kinase inhibitors sensitize prostate cancer cells to apoptosis triggered by Bcl-2 family inhibitor ABT-737. Cancer Res *72*, 294–303.

Spivak, J.L. (2002). Polycythemia vera: myths, mechanisms, and management. Blood *100*, 4272–4290.

Stiles, C.D., and Rowitch, D.H. (2008). Glioma stem cells: a midterm exam. Neuron *58*, 832–846.

Stoecklin, G., Gross, B., Ming, X.-F., and Moroni, C. (2003). A novel mechanism of tumor suppression by destabilizing AU-rich growth factor mRNA. Oncogene *22*, 3554–3561.

Stoecklin, G., Stubbs, T., Kedersha, N., Wax, S., Rigby, W.F.C., Blackwell, T.K., and Anderson, P. (2004). MK2-induced tristetraprolin:14-3-3 complexes prevent stress granule association and ARE-mRNA decay. The EMBO Journal *23*, 1313–1324.

Su, Y.-L., Wang, S.-C., Chiang, P.-Y., Lin, N.-Y., Shen, Y.-F., Chang, G.-D., and Chang, C.-J. (2012). Tristetraprolin Inhibits Poly(A)-Tail Synthesis in Nuclear mRNA that Contains AU-Rich Elements by Interacting with Poly(A)-Binding Protein Nuclear 1. PLoS ONE *7*, e41313.

Sun, C., Cai, M., Gunasekera, A.H., Meadows, R.P., Wang, H., Chen, J., Zhang, H., Wu, W., Xu, N., Ng, S.C., et al. (1999). NMR structure and mutagenesis of the inhibitor-of-apoptosis protein XIAP. Nature *401*, 818–822.

Sun, C., Cai, M., Meadows, R.P., Xu, N., Gunasekera, A.H., Herrmann, J., Wu, J.C., and Fesik, S.W. (2000). NMR structure and mutagenesis of the third Bir domain of the inhibitor of apoptosis protein XIAP. J Biol Chem *275*, 33777–33781.

Sun, L., Hui, A.-M., Su, Q., Vortmeyer, A., Kotliarov, Y., Pastorino, S., Passaniti, A., Menon, J., Walling, J., Bailey, R., et al. (2006). Neuronal and glioma-derived stem cell factor induces angiogenesis within the brain.

Cancer Cell *9*, 287–300.

Sun, L., Stoecklin, G., Van Way, S., Hinkovska-Galcheva, V., Guo, R.-F., Anderson, P., and Shanley, T.P. (2007). Tristetraprolin (TTP)-14-3-3 complex formation protects TTP from dephosphorylation by protein phosphatase 2a and stabilizes tumor necrosis factor-alpha mRNA. J Biol Chem *282*, 3766–3777.

Suswam, E., Li, Y., Zhang, X., Gillespie, G.Y., Li, X., Shacka, J.J., Lu, L., Zheng, L., and King, P.H. (2008). Tristetraprolin down-regulates interleukin-8 and vascular endothelial growth factor in malignant glioma cells. Cancer Res *68*, 674–682.

Takahashi, R., Deveraux, Q., Tamm, I., Welsh, K., Assa-Munt, N., Salvesen, G.S., and Reed, J.C. (1998). A single BIR domain of XIAP sufficient for inhibiting caspases. J Biol Chem *273*, 7787–7790.

Tamm, I., Kornblau, S.M., Segall, H., Krajewski, S., Welsh, K., Kitada, S., Scudiero, D.A., Tudor, G., Qui, Y.H., Monks, A., et al. (2000). Expression and prognostic significance of IAP-family genes in human cancers and myeloid leukemias. Clin Cancer Res *6*, 1796–1803.

Taylor, G.A. (1996). Mitogens stimulate the rapid nuclear to cytosolic translocation of tristetraprolin, a potential zinc-finger transcription factor. Mol Endocrinol *10*, 140–146.

Taylor, G.A., Carballo, E., Lee, D.M., Lai, W.S., Thompson, M.J., Patel, D.D., Schenkman, D.I., Gilkeson, G.S., Broxmeyer, H.E., Haynes, B.F., et al.

(1996). A pathogenetic role for TNF alpha in the syndrome of cachexia, arthritis, and autoimmunity resulting from tristetraprolin (TTP) deficiency. Immunity *4*, 445–454.

Taylor, G.A., Thompson, M.J., Lai, W.S., and Blackshear, P.J. (1995). Phosphorylation of tristetraprolin, a potential zinc finger transcription factor, by mitogen stimulation in intact cells and by mitogen-activated protein kinase in vitro. J Biol Chem *270*, 13341–13347.

Tchen, C.R. (2004). The Stability of Tristetraprolin mRNA Is Regulated by Mitogen-activated Protein Kinase p38 and by Tristetraprolin Itself. Journal of Biological Chemistry *279*, 32393–32400.

Tenev, T., Bianchi, K., Darding, M., Broemer, M., Langlais, C., Wallberg, F., Zachariou, A., Lopez, J., MacFarlane, M., Cain, K., et al. (2011). The Ripoptosome, a Signaling Platform that Assembles in Response to Genotoxic Stress and Loss of IAPs. Mol Cell *43*, 432–448.

van Oosten, A.L., Costa, Y., Smith, A., and Silva, J.E.C.R. (2012). JAK/STAT3 signalling is sufficient and dominant over antagonistic cues for the establishment of naive pluripotency. Nature Communications *3*, 817–12.

Vandenabeele, P., Galluzzi, L., Berghe, T.V., and Kroemer, G. (2010). Molecular mechanisms of necroptosis: an ordered cellular explosion. Nat Rev Mol Cell Biol *11*, 700–715.

Vanlangenakker, N., Vanden Berghe, T., and Vandenabeele, P. (2012). Many stimuli pull the necrotic trigger, an overview. Cell Death Differ *19*, 75–

86.

Varnum, B.C., Ma, Q.F., Chi, T.H., Fletcher, B., and Herschman, H.R. (1991). The TIS11 primary response gene is a member of a gene family that encodes proteins with a highly conserved sequence containing an unusual Cys-His repeat. Mol Cell Biol *11*, 1754–1758.

Vellanki, S.H.K., Grabrucker, A., Liebau, S., Proepper, C., Eramo, A., Braun, V., Boeckers, T., Debatin, K.-M., and Fulda, S. (2009). Small-molecule XIAP inhibitors enhance gamma-irradiation-induced apoptosis in glioblastoma. Neoplasia *11*, 743–752.

Venere, M., Fine, H.A., Dirks, P.B., and Rich, J.N. (2011). Cancer stem cells in gliomas: identifying and understanding the apex cell in cancer's hierarchy. Glia *59*, 1148–1154.

Vercammen, D., Beyaert, R., Denecker, G., Goossens, V., Van Loo, G., Declercq, W., Grooten, J., Fiers, W., and Vandenabeele, P. (1998). Inhibition of caspases increases the sensitivity of L929 cells to necrosis mediated by tumor necrosis factor. J Exp Med *187*, 1477–1485.

Vignudelli, T., Selmi, T., Martello, A., Parenti, S., Grande, A., Gemelli, C., Zanocco-Marani, T., and Ferrari, S. (2010). ZFP36L1 negatively regulates erythroid differentiation of CD34+ hematopoietic stem cells by interfering with the Stat5b pathway. Mol Biol Cell *21*, 3340–3351.

Vince, J.E., Wong, W.W.-L., Khan, N., Feltham, R., Chau, D., Ahmed, A.U., Benetatos, C.A., Chunduru, S.K., Condon, S.M., McKinlay, M., et al. (2007).

IAP antagonists target cIAP1 to induce TNFalpha-dependent apoptosis. Cell *131*, 682–693.

Weller, M., Stupp, R., Reifenberger, G., Brandes, A.A., van den Bent, M.J., Wick, W., and Hegi, M.E. (2010). MGMT promoter methylation in malignant gliomas: ready for personalized medicine? Nat Rev Neurol *6*, 39–51.

Wilusz, C.J., and Wilusz, J. (2004). Bringing the role of mRNA decay in the control of gene expression into focus. Trends in Genetics *20*, 491–497.

Xie, T.-X., Xia, Z., Zhang, N., Gong, W., and Huang, S. (2010). Constitutive NF-kappaB activity regulates the expression of VEGF and IL-8 and tumor angiogenesis of human glioblastoma. Oncol Rep *23*, 725–732.

Xie, Y., Xu, K., Dai, B., Guo, Z., Jiang, T., Chen, H., and Qiu, Y. (2006). The 44 kDa Pim-1 kinase directly interacts with tyrosine kinase Etk/BMX and protects human prostate cancer cells from apoptosis induced by chemotherapeutic drugs. Oncogene *25*, 70–78.

Young, L.E., Sanduja, S., Bemis-Standoli, K., Pena, E.A., Price, R.L., and Dixon, D.A. (2009). The mRNA binding proteins HuR and tristetraprolin regulate cyclooxygenase 2 expression during colon carcinogenesis. Gastroenterology *136*, 1669–1679.

Zanocco-Marani, T. (2010). TIS11/TTP gene family: It's never too late for tumor suppressors. Cell Cycle *9 (24)* 1-1.

Ziegler, D.S., Wright, R.D., Kesari, S., Lemieux, M.E., Tran, M.A., Jain, M.,

Zawel, L., and Kung, A.L. (2008). Resistance of human glioblastoma multiforme cells to growth factor inhibitors is overcome by blockade of inhibitor of apoptosis proteins. Journal of Clinical Investigation *118*, 3109–3122.